AD NUMBER

AD808503

NEW LIMITATION CHANGE

TO

Approved for public release, distribution unlimited

FROM

Distribution authorized to U.S. Gov't. agencies and their contractors; Administrative/Operational Use; 1 Mar 1967. Other requests shall be referred to Air Force Technical Applications Center, Patrick AFB, FL.

AUTHORITY

USAF ltr, 25 Jan 1972

DETECTION OF SURFACE WAVES FROM SMALL EVENTS AT TELESEISMIC DISTANCES

1 March 1967

Prepared For

AIR FORCE TECHNICAL APPLICATIONS CENTER

Washington, D. C.

By

S. S. Alexander

THE PENNSYLVANIA STATE UNIVERSITY

D. B. Rabenstine

EARTH SCIENCES DIVISION
TELEDYNE INDUSTRIES, INC.

DETECTION OF SURFACE WAVES

FROM SMALL EVENTS AT TELESEISMIC DISTANCES

SEISMIC DATA LABORATORY REPORT NO. 175

AFTAC Project No:	VELA T/6702
Project Title:	Seismic Data Laboratory
ARPA Order No:	624
ARPA Program Code No:	5810
Name of Contractor:	EARTH SCIENCES DIVISION TELEDYNE INDUSTRIES, INC.
Contract No:	AF 33(657)-15919
Date of Contract:	18 February 1966
Amount of Contract:	$ 1,842,884
Contract Expiration Date:	17 February 1967
Project Manager:	William C. Dean (703) 836-7644

P. O. Box 334, Alexandria, Virginia

<u>AVAILABILITY</u>

This document is subject to special export controls and each transmittal to foreign governments or foreign national may be made only with prior approval of Chief, AFTAC.

TABLE OF CONTENTS

TABLE OF CONTENTS

(Continued)

LIST OF ILLUSTRATIONS

DETECTION OF SURFACE WAVES FROM SMALL EVENTS AT TELESEISMIC DISTANCES

ABSTRACT

A matched filter approach for distinguishing weak teleseismic
surface wave signals from background noise is presented. The method
discriminates against events not located in a particular source re-
gion of interest and provides estimates of magnitude and radiation
pattern, when a number of recording stations are available. Test
cases and typical results for different source regions are discussed.

INTRODUCTION

One of the important measures of source mechanism is the ex-
citation of surface waves. This encompasses such estimates as total
energy, radiation pattern, frequency spectrum, and radiation of Love
wave energy relative to Rayleigh wave energy. At one time or another
practically all of these estimates have been applied in the study of
large magnitude events. However, because the surface waves from
small events ($M \leq 5$) usually arrive at teleseismic distances with
amplitudes at or below the noise level, special techniques must be
employed to extract the desired information. We present here a
matched filter approach for detecting small amplitude surface waves,
estimating their total energy content, and determining their radia-
tion pattern. Results for several test cases and several events are
shown, to demonstrate the usefulness of this approach as well as
some of its limitations.

METHOD

Basically the matched filter approach amounts simply to
searching a record $x(t)$ for a known waveform $y(t)$. In particular,

it is assumed that $x(t) = ay(t) + n(t)$ where $\underline{a}$ is a constant and $n(t)$ is a random noise process. If no further assumptions are made with regard to the nature of the noise process, one can determine the least-squares estimate of $\underline{a}$ which minimizes $J(a,\tau) = \sum [x(t + \tau) - a\, y(t)]^2$ where the summation is over the length of $y(t)$. In the test series x, which is of longer duration than y, the lag τ indicates at what point in x the comparison is begun. The value of $\underline{a}$ obtained by setting $\frac{\partial J}{\partial a} = 0$ is

$$\hat{a} = \sum_{t} x(t + \tau)\, y(t) / \sum_{t} y^2(t) \tag{1}$$

Thus, the matched filter in this case is simply the waveform $y(t)$ and the matched filter output at lag τ is

$$\sum x(t + \tau)\, y(t) = Cxy\,(\tau) \tag{2}$$

The coherency at lag τ is given by

$$C(\tau) = \sum_{t} x(t + \tau)\, y(t) / \left[\sum_{t} x^2(t + \tau) \cdot \sum_{t} y^2(t) \right]^{\frac{1}{2}} \tag{3}$$

It always is bounded by $-1 \le C(\tau) \le 1$. The maximum in the envelope of $C(\tau)$ occurs at the value of τ where x and y match best in the least-squares sense. This $C_{max}(\tau)$ is the correlation coefficient.

In the present application we have used this simple least squares approach. Estimates of $\underline{a}$, $C_{xy}(\tau)$, and $C(\tau)$ calculated in this way allow us to study test cases and unknown events with a minimum of assumptions.

A further refinement in the method can be made, however, if the noise is a stationary random process whose correlation matrix R can be calculated. If the sampled x(t) and y(t) are considered as row vectors, x and y, then an estimate of a is given by

$$\hat{a} = xR^{-1} y' / yR^{-1} y' \qquad (4)$$

where the prime denotes transpose. This is the maximum likelihood estimate of a. In this case $R^{-1} y'$ is the filter. (Details of the statistical analysis leading to these estimates are given in Chapter II of Reference 1).

This modified approach may allow us to do a better job in detecting events, since it accounts for the noise as well as the known waveform. However, we have not yet investigated its usefulness sufficiently to determine whether the extra computation required to calculate the correlation matrix of the noise is warranted.

In the least-squares approach we chose the following decision criteria to determine whether or not a signal was present:

1. A relative maximum in the envelope of $C(\tau)$ must fall in the expected time window based on travel-time information.

2. This value of $C_{max}(\tau)$ must be greater than or at least comparable to typical peak values in the envelope of $C(\tau)$ outside the expected time window.

3. An arrival must be detected within the proper expected time window at each of several stations.

If all three of these criteria were met, then the signal was considered to be present.

IMPLEMENTATION

The matched filter approach just discussed requires that one knows the desired or expected waveform in order to search effectively for that waveform in a noisy record. In order to obtain a suitable "expected" waveform and at the same time assure that propagation effects would be properly accounted for, we chose the surface wave from a larger event in the source region of interest as the filter $y(t)$. Thus, no matter how complicated the paths of propagation are, the paths for other events in the same source region will be nearly coincident with those of the larger event which produced $y(t)$, so the only major differences in recorded waveform will be source differences. This situation is illustrated schematically in Figure 1, which shows the surface wave trajectories appropriate for a source region in the ocean and a continental recording station.

This coincidence of travel path simply assures that the earth's transfer function is the same for all events occurring in that source region; it does _not_ mean that dispersion during propagation to teleseismic distances is unimportant. To the contrary, it is this physical effect (dispersion) which is vital to the success of the technique, since it transforms the source pulse into an oscillatory signal which is of long duration. As the duration of the signal increases, random correlations of the signal with the noise become poorer, with the result that the "false alarm" level is reduced. From this standpoint the larger the epicentral distance the better the method should work, since the signal increases in duration the larger the distance. However, the energy density of the signal is reduced due to dispersion and attenuation

- 4 -

during propagation, so that the signal to noise ratio is reduced with increasing distance. Therefore, for a given transfer function and noise level, one would expect there to be an optimum observing distance for detecting events using the matched filter. But, because of the different noise levels among available stations and the variety of propagation paths to these stations, it does not appear to be practical to determine these optimum observing distances experimentally. What we can estimate, however, is the minimum S/N at which the technique will detect observed or expected signal waveforms.

Because of dispersion and frequency-dependent attenuation with distance, the signal waveform will in general be different at each station and thus a different filter for each station and source region must be used. However, this presents no problem since a single large event in a given source region provides for each station a filter suitable for detecting other events located in that region, as well as the temporal pattern of arrival times at the stations. This pattern and the fact that the filters are different for each station can be used to advantage in discriminating against events outside the source region of interest, since one or more of the decision criteria listed earlier will not be satisfied; in particular, the correlation peak values will be degraded, and the arrival times of these peaks will not produce the appropriate pattern of arrival times at the observing stations.

When a small event has been detected by this method, then the question arises as to what details we can extract about the source. The estimates of a provide a convenient means of comparing the magnitude of the small event to that of the larger one, since a^2 is an estimate of the ratio of the energy in the small event to

- 5 -

that in y(t). Some care must be taken, however, if the reference
event exhibits a strong radiation pattern which is different from
that of the smaller event. In fact, the radiation pattern of the
small event relative to the reference event can be obtained by
plotting $\hat{a}/\Sigma_t y^2(t)$ vs. source-station azimuth.

Comparisons of $\hat{a}$ vs. distance along a given azimuth allow
us to estimate roughly the excitation spectrum of the small event
compared to the larger one, since the attenuation with distance is
frequency-dependent, which implies that $\hat{a}$ should vary with distance
in a way which reflects the shape of the spectrum of the small event
compared with that of the reference event. Only if their spectra are
identical in shape will $\hat{a}$ be invariant with distance. Since this at-
tenuation factor is of the form $\exp[-g(\omega)\Delta]$, where $g(\omega)$ is an in-
creasing function of frequency and Δ is epicentral distance, $\hat{a}$ will
decrease with distance if the spectrum of the small event is peaked
at a higher frequency than the reference event. A method for cal-
culating the spectrum of the small event relative to that of the
reference event is given in Appendix I.

Thus potentially the matched filter method permits us to:

1. detect the surface waves from a source region of interest,
while rejecting events outside the source region;

2. make magnitude estimates for small events relative to
the reference event;

3. outline radiation patterns for small events;

4. estimate spectral shape relative to the reference event.

Computer programs were written to implement the method along
the lines discussed above.

- 6 -

TEST CASES

In order to test the effectiveness and sensitivity of the
matched filter approach for surface waves, several test cases
were investigated.

Case I - Known signal added to actual noise at different signal-to-noise (S/N) ratios

Figure 2 shows the results of adding the signal shown at the
top (an actual oceanic Rayleigh wave train recorded at 4686 km
distance) to the noise trace at a number of arrival times, with the
indicated signal/noise, S/N, and using the signal as the matched
filter. We define S/N as $\max_t |y(t)|/\text{RMS}[n(t)]$. The number in
parentheses is an alternate value of signal/noise (S/N) given by
$\text{RMS}[y(t)]/\text{RMS}[n(t)]$. The values of $\alpha = \hat{a}$ are printed next to
C_{xy} trace, and the correlation coefficients CC next to the C trace.
The arrows indicate the beginning time for the signal in each in-
stance. In this example the signal is detected for S/N (S/N) as
low as .35 (.15), where visual detection is impossible. Notice
also that the $\hat{a}$'s are approximately in proportion to the S/N used
as expected.

The reason the results appear to be as good or better for
S/N = .35 compared to S/N = .5 is that the noise level was not
uniform over the entire noise trace used to establish the RMS of
the noise and the .35 signal was buried at a position where the
actual noise level over the filter length was low relative to that
where the .5 signal was buried.

Case II - Same as Case I with different signal and noise.

Figure 3 shows the results when a different signal (a
synthetic seismogram calculated for an assumed dispersion curve)
is added to the noise at different levels. The format is the
same as in Figure 2. This signal waveform approximates that for
a purely continental propagation path with the dispersion shown
in Figure 4. We can detect this signal down to a S/N of about
.4 (.14), which is again considerably below the threshold of
visual detection. This noise sample was identical to that used
in Case I, so the same comments hold with regard to how well the
signal is detected at different positions. These cases, along with
results for other test cases, suggest that if the signal buried in
the noise is identical in waveform to the reference event, it can be
detected when the S/N is above about .35 (.15) and that the $\hat{a}$'s pro-
vide reliable measures of the relative amplitudes of the two events
down to a S/N of about .5. It should be noted that the indicated
$\hat{a}$ values include a gain factor introduced in constructing a partic-
ular S/N level in the x(t) trace using y(t) and a given n(t).

Case III - Effects of varying epicentral distance

In order to test the sensitiveness of the method to pertur-
bations in source distance, we wrote a computer program to syn-
thesize the surface train to be expected at any distance for a
given phase velocity dispersion curve and amplitude spectrum
(see Appendix II). Using the dispersion curve shown in Figure 4
and the amplitude spectrum labeled A_0 in Figure 7, we synthesized
seismograms for distances in the range from 3000 to 4000 km, in
50-km increments. Figure 5 shows some of these synthetic records
and the corresponding matched filter results, when the seismogram

- 8 -

at 3000 km was used as the reference in each case and no noise was present. The values of $\hat{a}$ and CC are a measure of the effect of distance perturbations on the matched filter response. Surprisingly perhaps, the method appears to be rather insensitive to changes in source distance; this is indicated in Figure 6 where the correlation coefficients are plotted vs. differences in epicentral distance. Since the group velocity window and amplitude spectra were kept fixed in this case the values of $\hat{a}$ and CC are identical. There is the expected decrease, but the correlation coefficient is above .8 for distance differences as large as 1000 km. It should be pointed out that this result is not independent of the assumed dispersion and amplitude spectrum. That is, a given perturbation in distance will produce a change in signal waveform which depends on both the dispersion in the source region and the amplitude spectrum. Nevertheless, this case is probably sufficiently representative to infer that the method does not depend critically on the closeness cf the reference source to the source of interest insofar as the correlations are concerned. This was borne out in the analysis of actual events. However, the relative travel-time pattern would still require the events to be rather close together, since, for example, a 100-km difference could result in relative arrival time shifts among stations of as much as 25-30 seconds.

Case IV - Effects of amplitude spectra on matched filter response

Differences in the amplitude spectrum of the reference event compared to the test event can be expected, since in general the lower the magnitude the higher the frequency of the peak in the

amplitude spectrum observed at a given distance. Thus, when we look for small events using large ones we almost certainly are not dealing with spectra which are similar either in shape or position in frequency. To test these effects we computed the matched filter response for the synthetic seismograms corresponding to the amplitude spectra shown in Figure 7. The dispersion used was the same as for Case III; the distance was taken as 3000 km, and the reference spectrum is the one labeled A_0 in Figure 7. The matched filter results are shown in Figure 8. In this case the effect on both $\hat{a}$ and the correlation coefficient is more pronounced, as shown in Figure 9. One reason that $\hat{a}$ and CC do not coincide is that only energy in a fixed group velocity window is included in the synthesis, so the relative energies may differ from one calculation to another. In any case our estimates of $\hat{a}$ and CC are apt to be lowered if the excitation spectra are different. On this basis it would be desirable to use smaller magnitude events for reference sources, but if this is done then the reference signal itself is degraded by noise. We conclude from visual examination of the teleseismic Rayleigh waves from a number of events that earthquakes in the body wave magnitude range 5.5-6.0 usually have a high enough S/N to be usable as reference events. Some lower magnitude earthquakes also exhibit large enough surface waves to be used for reference.

RESULTS

In this section we present some of the results of applying the matched filter approach discussed above to actual data. These results are intended primarily to demonstrate the practical applicability of the method, and no claims are made about a general minimum threshold of detection, although events as small as magnitude 4.1 were observed at teleseismic distances in some instances. Many more small events must be analyzed before the performance limits of the matched filter approach can be adequately assessed.

Results for three different source regions - Aleutians (Amchitka), Kamchatka, and Hawaii - are presented. The observation stations are LRSM stations or VELA Observatories in North America. The epicenter information for the three sets of events we discuss is given in Table I.

The organization in the figures to follow conforms to the standard format adopted for displaying all matched filter results for actual events. That is, a station set consists of four traces; the top trace is the signal y(t), the second trace is the observed seismogram x(t), the third trace is $C_{xy}(\tau)$, and the bottom trace is $C(\tau)$. The legend at the left gives values of distance, $\hat{a}$, and CC as well as station and event identification. The arrows indicate the location of the expected signal arrival at each station. This is where the peak in the matched filter output should occur; that is, the beginning point of y(t) in x(t). The interval between each time mark is 50 seconds unless otherwise indicated.

ALEUTIAN SOURCE REGION

Comparison of an explosion and an earthquake of comparable magnitude.

The explosion was LONGSHOT (body wave magnitude 5.97); the earthquake was a magnitude 5.9 event located within a degree of the

- 11 -

LONGSHOT site (see Table I). At each station the surface waves
from the 22 November 1965 earthquake were chosen as the reference
signal, and the LONGSHOT seismograms were scanned for surface waves
with the earthquake signal used as the matched filter. Some of the
results for Rayleigh waves are shown in Figure 10.

It is seen that the Rayleigh wave was clearly detected at
all but one station. The Rayleigh wave amplitude of LONGSHOT rel-
ative to that of the magnitude 5.9 earthquake, however, is below .12
everywhere in the distance range analyzed (3500-7000 km). This
means that the surface wave magnitude for LONGSHOT is only about 5.0
if the surface wave magnitude of the reference earthquake is equiva-
lent to its body wave magnitude. It also means that the R/P exci-
tation for the explosion is nearly an order of magnitude smaller
than the R/P excitation for an equivalent size earthquake.

The results in Figure 10 are for the vertical components only.
We did the same analysis for the radial components and got essentially
the same results. Therefore, these are not shown.

We also tried different signal durations for y(t) and found
that the signals shown in Figure 10 gave a better result (correlation)
than did longer signals which included part of the coda of the earth-
quake. This probably reflects the situation that in using the longer
filter more noise was included in the correlation interval for both
y(t) and x(t) without a proportional increase in signal energy in-
cluded in the interval.

Since the 22 November event also generated strong Love waves,
we used them as a matched filter to search the LONGSHOT seismograms
for Love waves in the same way we searched for Rayleigh waves. We
used the transverse components throughout. With the possible excep-
tion of two stations we were not able to detect any Love waves from
LONGSHOT. Therefore, in Figure 11 we show the results for only

three stations including the two where a Love wave arrival might
be indicated. The bottom set in Figure 11 is representative of
the stations where nothing was detected. The indicated values
of $\hat{a}$ in Figure 11 give an upper bound of about .01 for the ampli-
tude of Love waves for LONGSHOT relative to the Love waves for the
22 November earthquake. This result is not surprising, since an
examination of the short period seismograms for LONGSHOT reveals
that it was an explosion which excited shear waves poorly or not
at all.

In Figure 12 is shown a plot of $\hat{a}$ vs. distance for the
LONGSHOT Rayleigh waves observed along the azimuth shown in Figure
16. The observed values of $\hat{a}$ decrease with distance which indicates
that the spectrum of LONGSHOT Rayleigh waves is peaked at higher
frequencies than is the 22 November earthquake spectrum (see Appen-
dix I). In all cases the values of $\hat{a}$ are below .12 indicating, as
mentioned before, a smaller Rayleigh wave magnitude for LONGSHOT.

Comparison of smaller magnitude earthquakes with the 22 November
1965 earthquake.

In order to concentrate on the smaller magnitude events in
the Amchitka area, we analyzed only a few events for intermediate
magnitudes of approximately 5, using only a few stations to verify
that the Rayleigh waves could be detected. The Rayleigh waves from
earthquakes of magnitude greater than 5 from this region can be
clearly seen visually on the film records, so the matched filter
analysis is not needed for detection of these events. Figure 13
shows the matched filter output for a single station for the mag-
nitude 4.9 event listed in Table I. The surface wave is clearly
detected.

In Figure 14 we show the matched filter results for the magnitude 4.0 earthquake (20 February 1966) listed in Table I. Notice that the source depth for this event was 48 km which means that the surface wave excitation is necessarily smaller than if the same source were located closer to the surface. From Figure 14 it appears that this event was barely detected at several stations but not detected at every station. The values of δ average about .01 which is approximately the value expected for a magnitude difference of 2. Certainly this event is at or near the lower limit of detectability using the matched filter approach.

From the limited analysis we have done, it would appear that we can detect earthquake events with magnitudes approaching 4 from the Amchitka region. Certainly the threshold is below magnitude 5. However, more small events must be analyzed before a lower magnitude threshold for detection can be firmly established.

KAMCHATKA SOURCE REGION

We present in this section results for the 5 events located in Kamchatka which are listed in Table I. In these cases the observing distances were in the range from 5300-8000 km which overlaps, but extends further than, the distances investigated for the Aleutian events. We consider only Rayleigh waves and use the Rayleigh waves from the 29 January 1965, magnitude 5.8 event as the matched filter in all cases. Note in Table I that all these events are located within 2-3 degrees of each other.

Analysis of the magnitude 5.3 event (20 April 1965)

Shown in Figure 15 are some of the matched filter results for this event. The event clearly was detected at all but 2 of the 20 stations analyzed. These two HL2ID and BLWV, are included in Figure 15.

- 14 -

They possibly define a node on the radiation pattern since they are
aligned approximately on a single azimuth from the source. Note
that at some stations the correlation coefficient for the arrival is
quite high ($>$ .6). Figure 16 is a map showing the observed values
of $(\hat{a})^{-1}$, that is, the amplitude of the large event relative to the
small one at the various stations. With the exception of the vicin-
ity of the suspected nodal line, the values of $(\hat{a})^{-1}$ are consistent
in each geographical area where several stations are clustered. For
the given USC&GS body wave magnitudes the value of $\hat{a}$ in this case
should be about .32 or equivalently its inverse should be about 3.1,
a somewhat lower value than actually observed at most stations. This
would suggest that the magnitude of the 20 April 1965 event is slightly
below 5.3. However, it must be remembered that the higher values of
$(\hat{a})^{-1}$ observed could also result from a different radiation pattern
or an excitation spectrum peaked at higher frequencies than the ref-
erence event. Therefore, the observed values are probably reasonable
for a magnitude 5.3 event.

Analysis of the magnitude 5.1 event (6 July 1965)

In Figure 17 are shown some of the matched filter results
for this event. It is clear from the high values of the correlation
coefficient that the event was positively detected. Moreover, the
values of $\hat{a}$ are also large, and one can, in fact, see the signal
above the noise on most of the seismograms in Figure 12. Visual
picks of the amplitude ratio for this event consistently gave larger
values of $\hat{a}$ than those machine picked. Thus, the 6 July 1965 event
seems to be .3 or less smaller in magnitude than the 29 January 1965
event, which means that the estimated surface wave magnitude of the
6 July 1965 event is greater than 5.5. Moreover, comparison of

Figures 15 and 17 indicates that the 6 July 1965 event was definitely larger than the magnitude 5.3 event on 20 April 1965. Therefore, the body and surface wave magnitude estimates for the 6 July 1965 event differ by at least 0.4, with the surface wave magnitude the larger.

Analysis of the magnitude 5.0 event (14 February 1965)

Shown in Figure 18 are some of the filter results for this event. The method apparently detects the event but at a time 30-50 seconds earlier than expected at each station. This probably results from the fact that this event was nearly 4 degrees closer than the reference event. The $\hat{a}$'s are consistent and average around 17 implying that the surface wave magnitude of this event is slightly more than one unit below that for the reference event, that is, somewhat below 4.8. Since the excitation spectrum of the small event probably peaks at a higher frequency than that of the reference event, it is expected (Appendix I) that the matched filter estimate of $\hat{a}$, hence magnitude, will decrease with increasing epicentral distance. Thus, the results for this case are reasonably consistent with the body wave magnitude of 5.0.

Analysis of the magnitude 4.4 event (21 January 1965)

Shown in Figure 19 are some of the matched filter results for the 21 January 1965 event. It should be noted that this was a deep focus event (119 km), hence equivalent to a smaller magnitude shallow event as far as Rayleigh wave excitation is concerned. It appears that this event was barely detected by the method with estimates of $\hat{a}$ around .03. This value gives a magnitude estimate of about 4.2 for the 21 January event. which seems large, considering the source depth of 119 km. In any case this event appears to define the threshold of detectability for the Kamchatka region.

- 16 -

HAWAIIAN SOURCE REGION

Results for two small events are presented for this source region. The magnitudes of these events are 4.4 and 4.1 respectively, while the reference event is the magnitude 5.3 event (11 October 1964) listed in Table I.

Analysis of the magnitude 4.4 event (7 January 1964)

Shown in Figure 20 are matched filter results for the 7 January 1964 event at several stations. Tne event was apparently detected, but the amplitude estimates are quite small (around .02) a factor of 5 smaller than expected if the event is truly of magnitude 4.4. The large oscillatory output later in the records of C_{xy} and C represents the correlation of the reference event with another large event located some 7000 km more distant in New Britain. This correlation is of long duration because the more distant event has dispersed a great deal more in propagating the additional 7000 km and the filter, therefore, "sees" a signal for a long time in $x(t)$. This example provides another illustration of the fact that the method is weakly dependent on the separation of the sources and that arrival time patterns must be used as additional constraints if we wish to detect only events from a particular source region of interest.

Analysis of the magnitude 4.1 event (13 August 1964)

In Figure 21 are shown the results for the shallow focus (11 km) magnitude 4.1 event of 13 August 1964. This event is apparently detected at most of the stations. However, the corresponding correlation coefficients and the estimates of $\hat{A}$ are small. The apparent magnitude of the small event is about 1.6 sma.   an the reference event. However, the filtering effect of oceanic propagation of Rayleigh waves will greatly attenuate periods shorter than about 15 seconds and as the peak in excitation shifts to shorter periods for the smaller magnitude events, this effect should cause very significant reductions in surface wave energy, hence reduce the matched filter

- 17 -

estimates of surface wave magnitude at teleseismic distances.
Nevertheless, we have been able to "see" events of magnitude 4.1
and 4.4 for the Hawaiian source area.

DISCUSSION

In the foregoing sections we have demonstrated experi-
mentally that the surface waves from small events can be detected
at teleseismic distances using a matched filter method and that
reasonable estimates of some source characteristics can be made.
What has not been demonstrated is the minimum threshold of detection
for the method. The underlying difficulty which always can affect
the estimated threshold seriously is that the body wave magnitudes
used as an absolute standard for comparing events may be badly in
error. A more reliable absolute measure of source strength is needed
to evaluate the performance of the matched filter in detecting actual
events.

One of the most useful features of the matched filter method is
that it permits one to make meaningful surface wave magnitude estimates
even when the signal to noise level is so low that one cannot visually
detect the presence of the signal. This means that the matched filter
method can be used to obtain reliable surface wave magnitude estimates
for events so small that meaningful AR estimates of magnitude (Ref-
erence 4) cannot be obtained.

Several possible improvements in the matched filter approach
can be made. One was discussed in the Method section, that of in-
cluding the noise correlation matrix to obtain maximum-likelihood
estimates of $\hat{a}$ instead of least squares estimates. Another is to
use empirically derived scaling functions to adjust the spectrum of
the reference event to match that generally expected for a small
magnitude event; this should improve the correlation between the

- 18 -

reference and test traces. Another is to phase equalize and sum
over an array of stations before applying the matched filter.
In fact there is no reason why one should not make use of all the
available noise suppression techniques before applying the matched
filter; this could improve the detection capability of the matched
filter significantly.

The indirect method presented in Appendix I for estimating
the spectrum of the small event has not been investigated experi-
mentally in more than the rudimentary way done for LONGSHOT. Since
being able to determine the frequency spectrum of such small events
would be of very great value in studying their source mechanisms,
the practical applicability of the indirect method should be ex-
plored further.

CONCLUSIONS

On the basis of this investigation we conclude that:

1. In principle the matched filter approach can be used:

(a) to detect weak surface wave signals for signal to
noise ratios as low as about 0.35;

(b) to make reliable relative magnitude estimates for
S/N as low as .5;

(c) to determine radiation pattern relative to a reference
event;

(d) to estimate the general shape of a small event's am-
plitude spectrum relative to that of the reference event.

2. The results presented for a number of actual events have
demonstrated the practical applicability and usefulness of the matched
filter approach in studying weak teleseismic surface waves.

3. The matched filter used in conjunction with the surface wave arrival time patterns appropriate for different source regions of interest allows one to discriminate against all but those events in the particular source region of interest.

4. Rayleigh waves produced by the LONGSHOT explosion were detected at teleseismic distances. The excitation of LONGSHOT Rayleigh waves, however, was an order of magnitude smaller than the Rayleigh wave excitation for an equivalent magnitude earthquake in the same region.

5. Love waves could not be detected for the LONGSHOT explosion.

6. Teleseismic surface wave signals could be detected for small earthquakes of body wave magnitude less than 5 in each of the three different source regions investigated. The actual lower limit for each region is still uncertain.

REFERENCES

1. Simpson, S.M., et al, "Studies in Optimum Filtering of Single
    and Multiple Stochastic Processes," MIT Scientific Report
    No. 7 of Contract AF19(604)-7378, June 30, 1963.

2. Aki, K., "Study of Earthquake Mechanism by a Method of Phase
    Equalization Applied to Rayleigh and Love Waves,"
    J. Geophys. Res., Vol. 65, No. 2, 1960, pgs. 729-740.

3. Alexander, S., "Surface Wave Propagation in the Western United
    States", Ph.D. Thesis, California Institute of Technology,
    1963.

4. Brune, J., Espinosa, A., and Oliver, J., "Relative Excitation
    of Surface Waves by Earthquakes and Underground Explosions
    in the California-Nevada Region," J. Geophys. Res., Vol. 68,
    No. 11, 1963, pgs. 3501-3513.

5. Archambeau, C.B., "Elastodynamic Source Theory," Ph.D. Thesis,
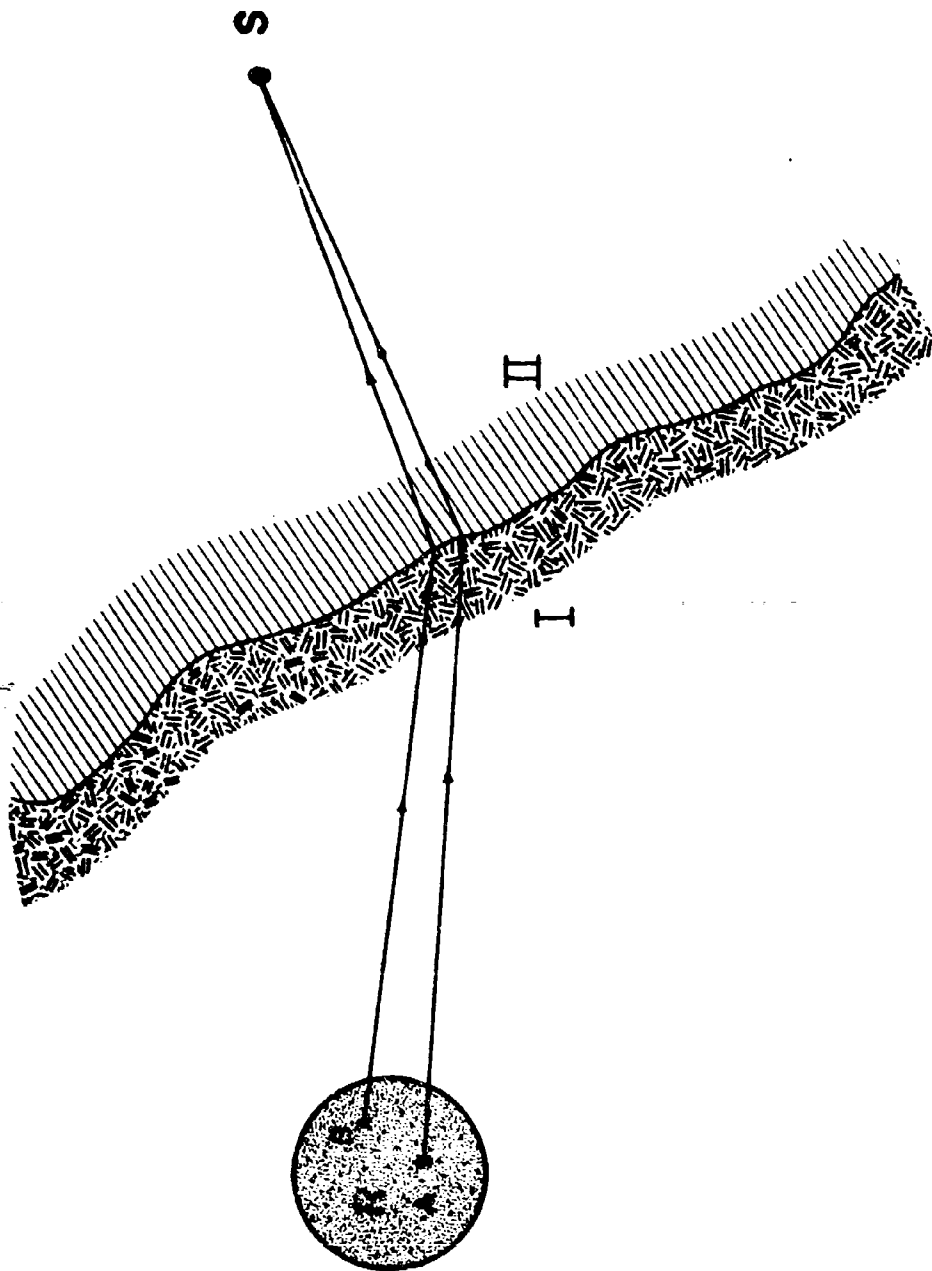   California Institute of Technology, 1964.

Figure 1. Schematic Map Showing Source Region R and Trajectories of Surface Waves (of a Particular Frequency) from Events A and B to an Observation Point S. Region I has a Higher Phase Velocity than Region II in this Hypothetical Case.
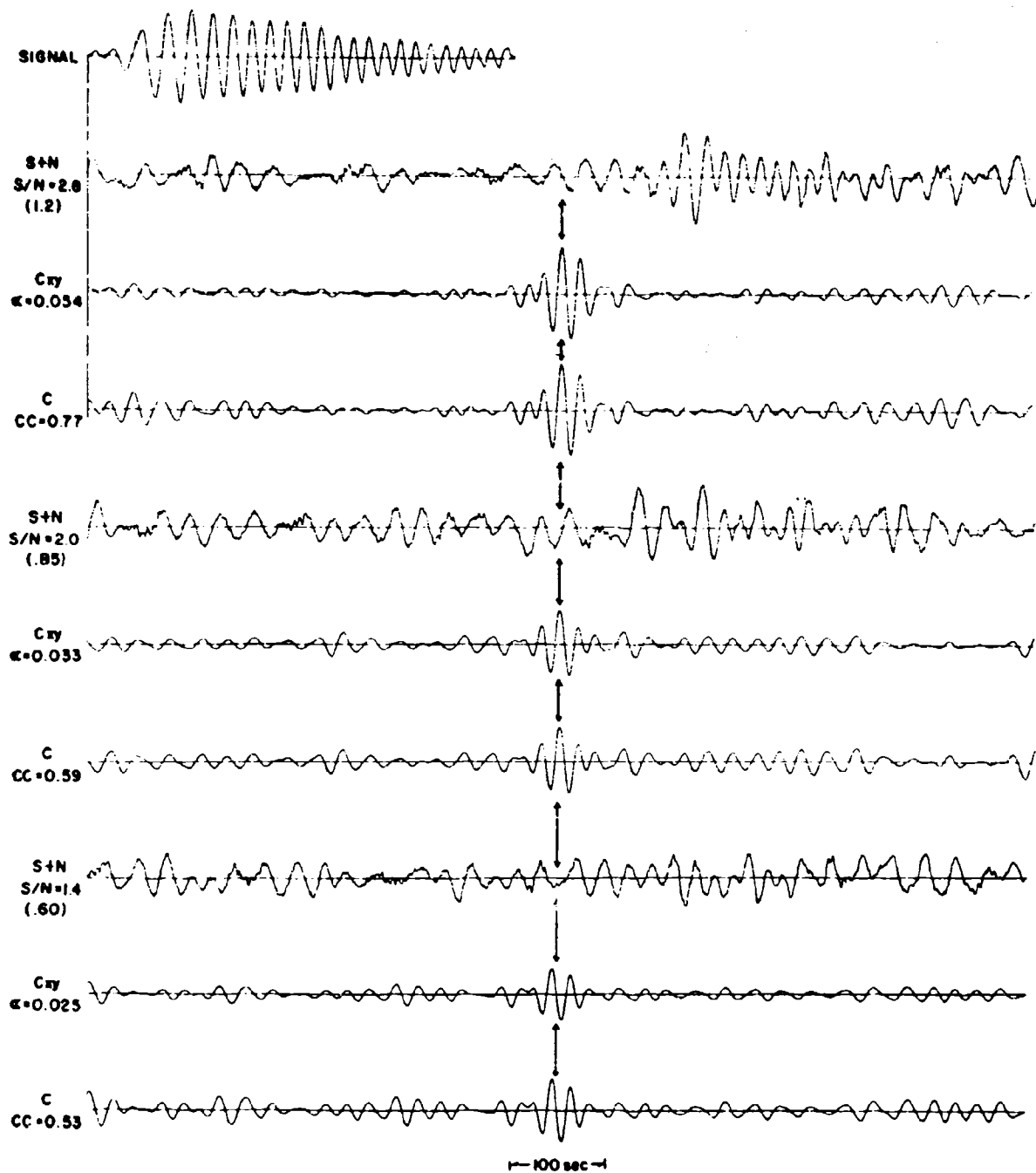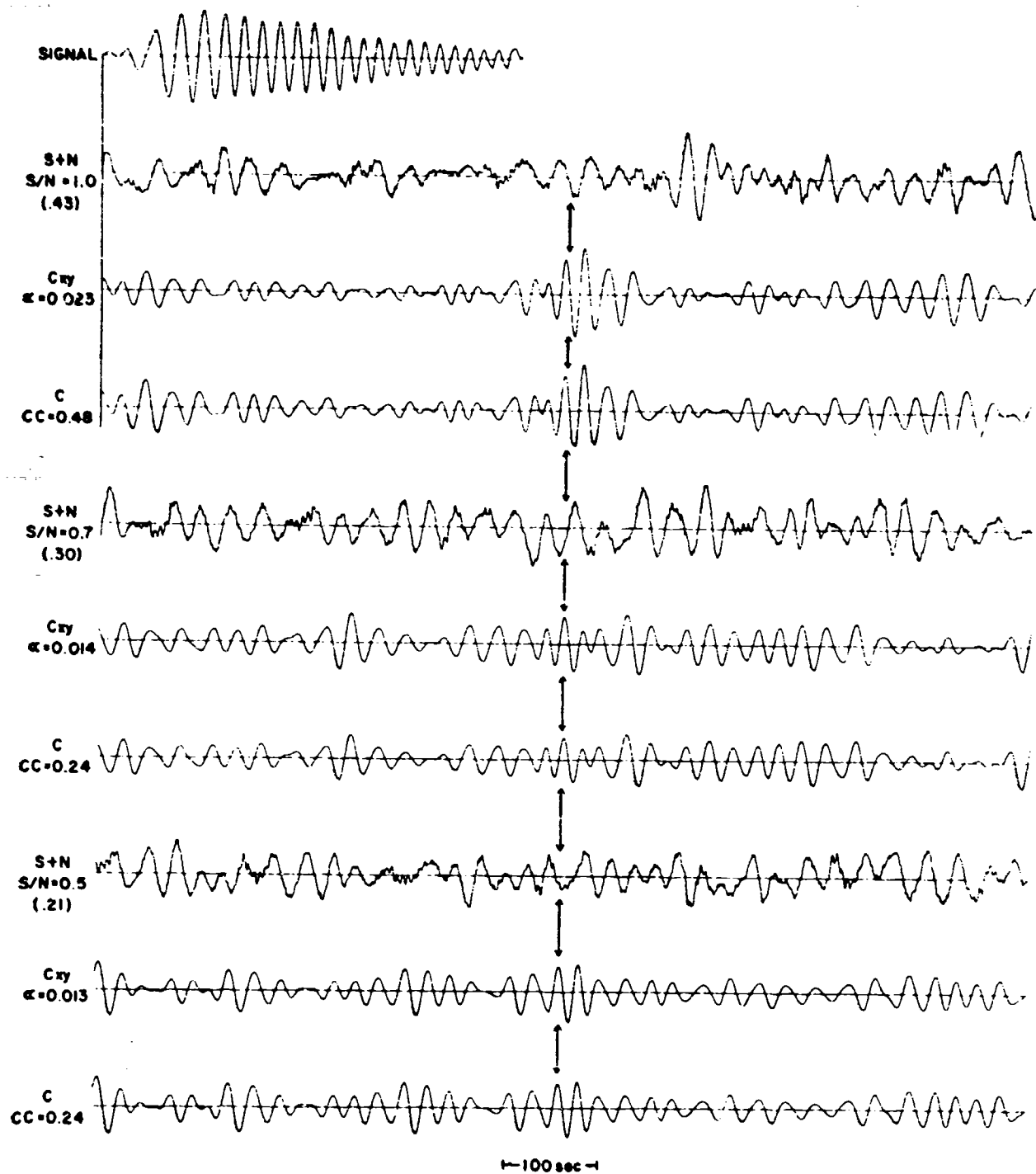
Figure 2A.   Real Signal Test Case
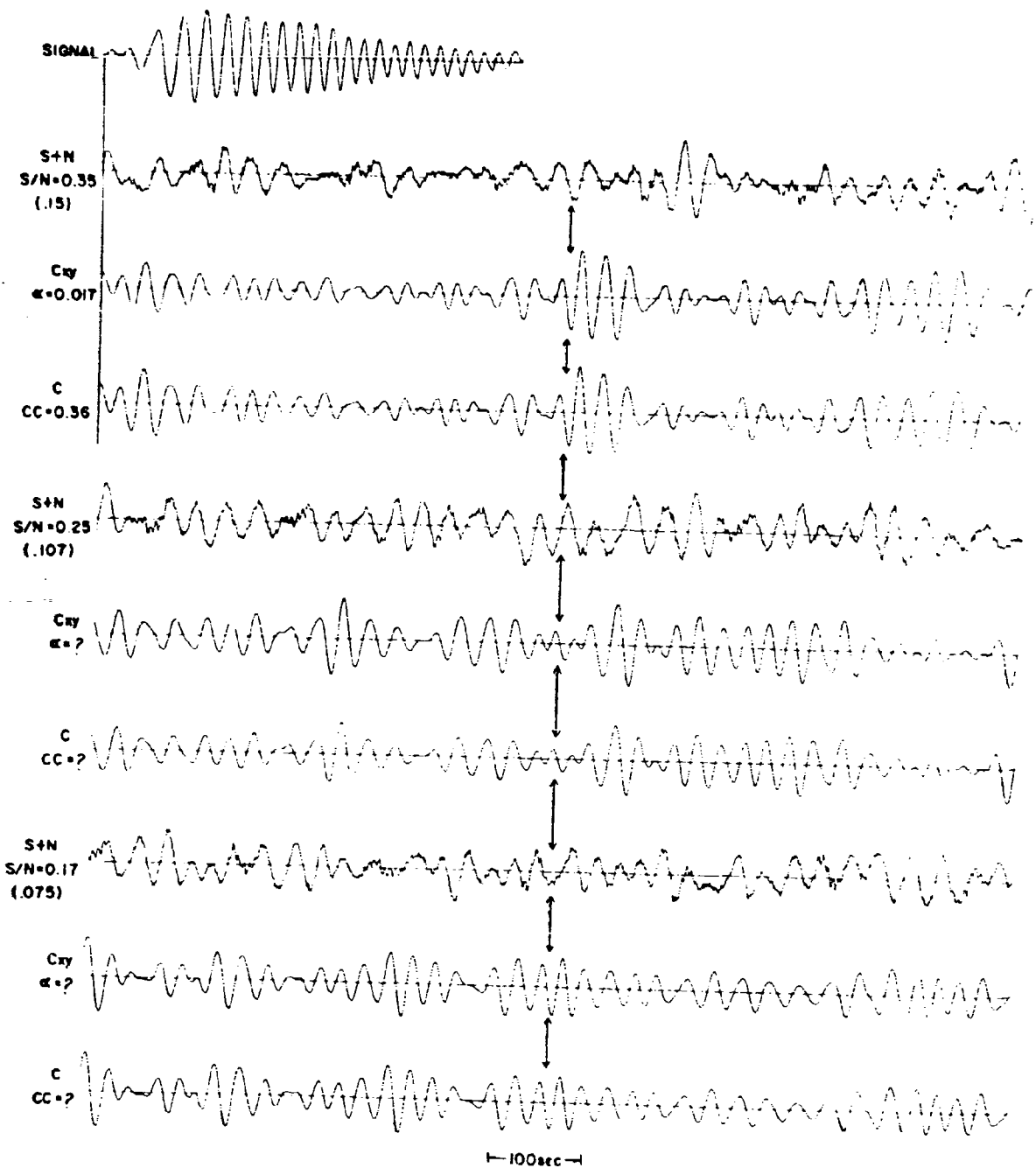
Figure 2B. Real Signal Test Case
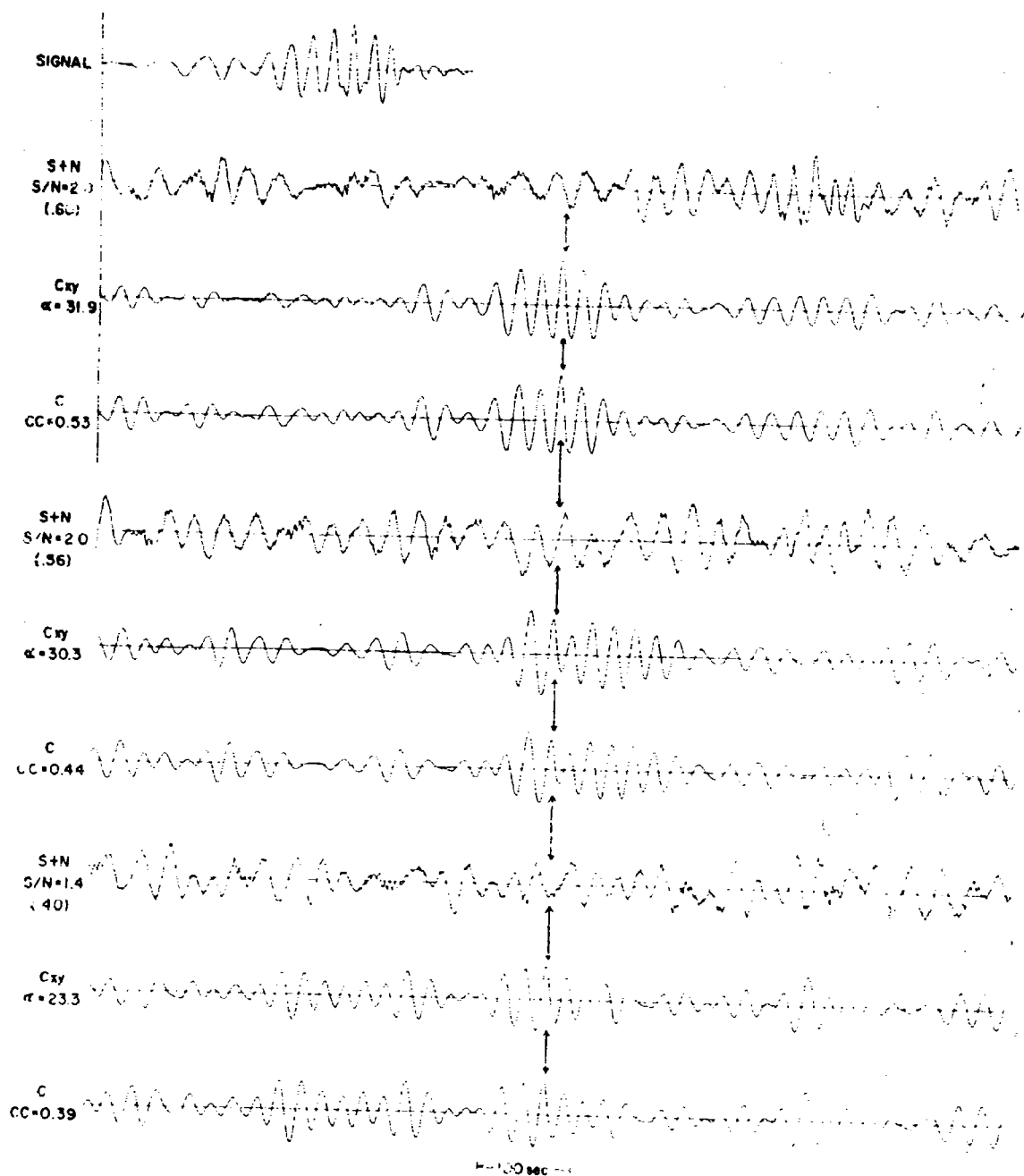
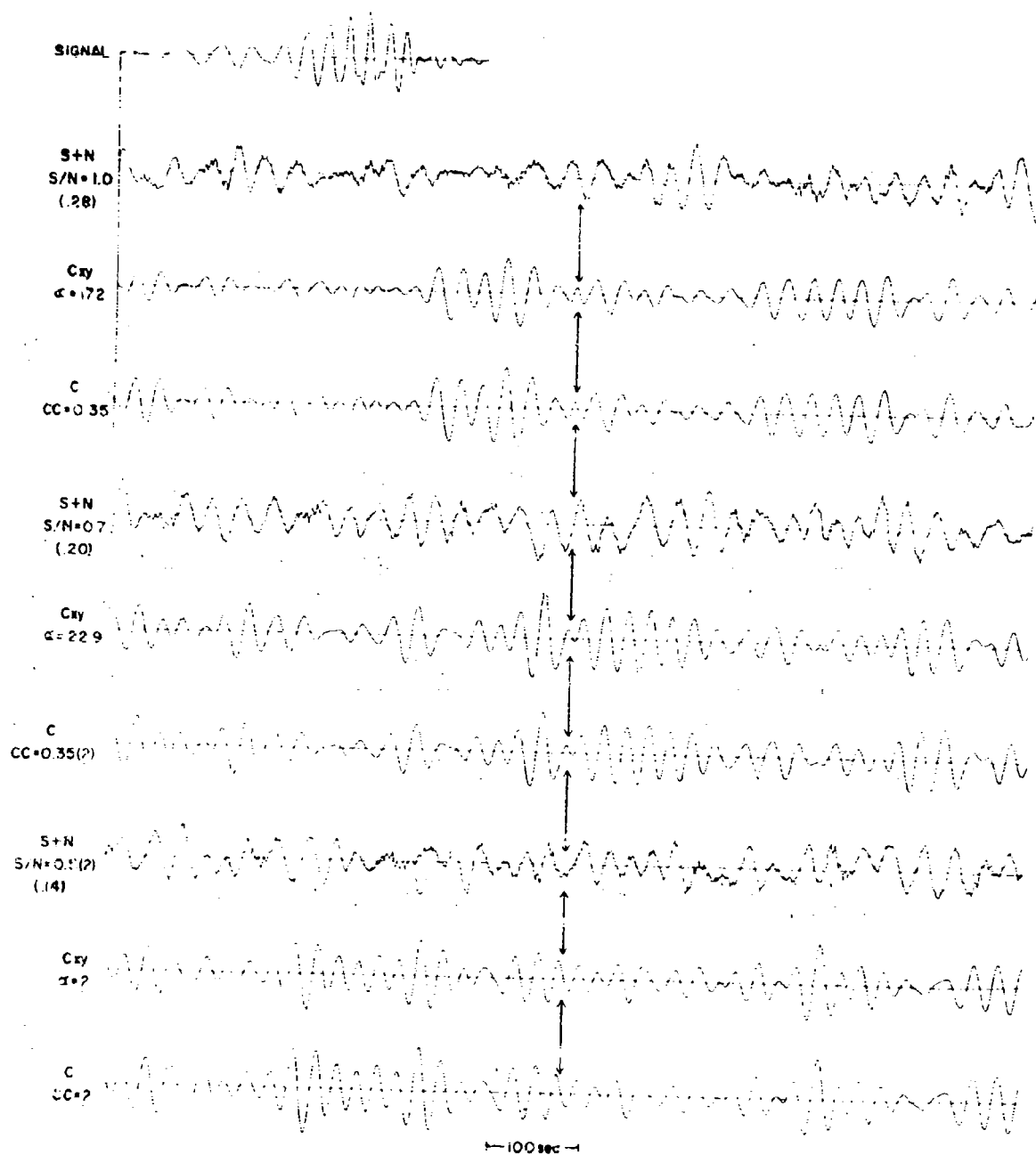Figure 2C. Real Signal Test Case

Figure 3A. Synthetic Signal Test Case

Figure 3B. Synthetic Signal Test Case
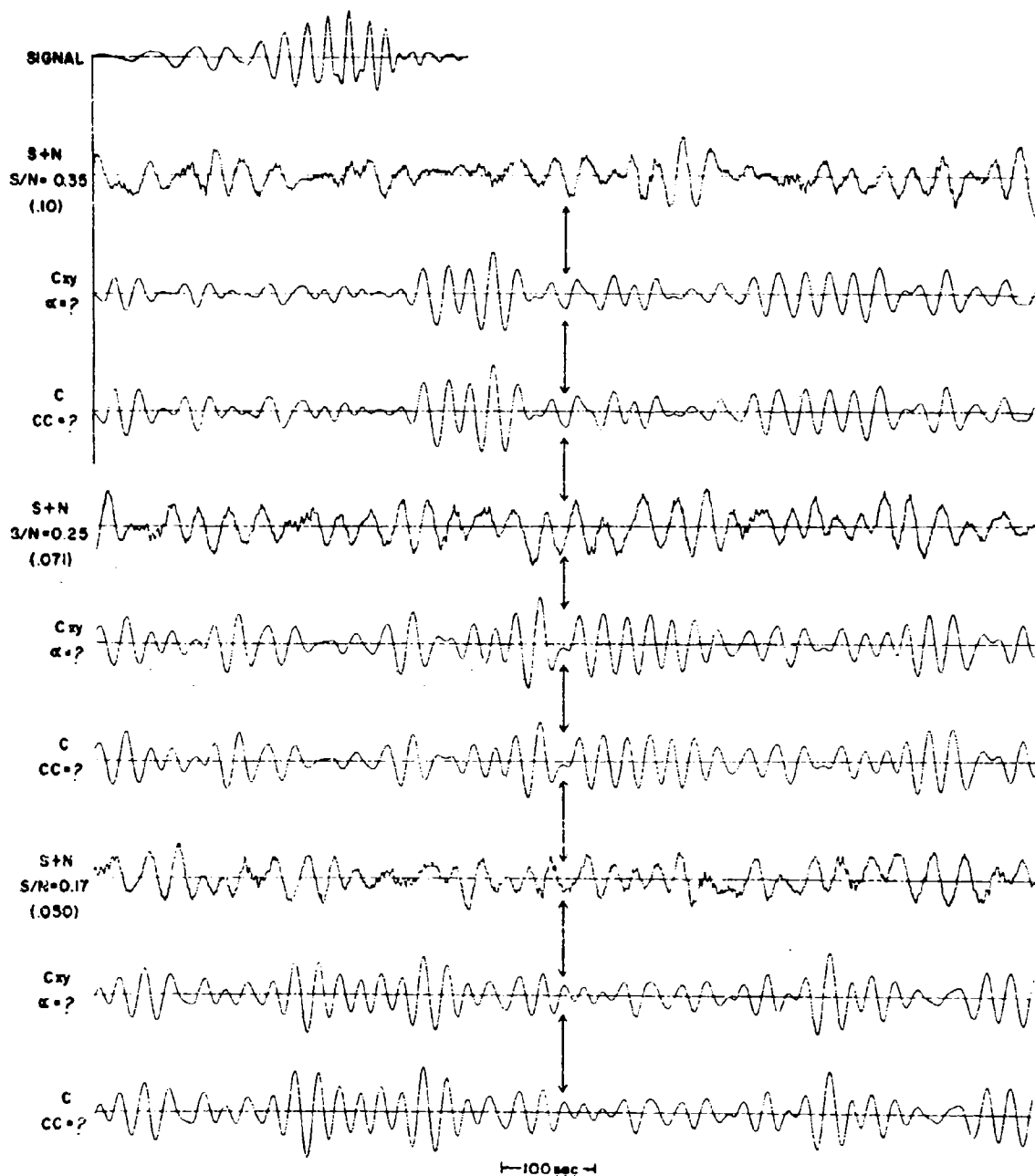
Figure 3C.   Synthetic Signal Test Case
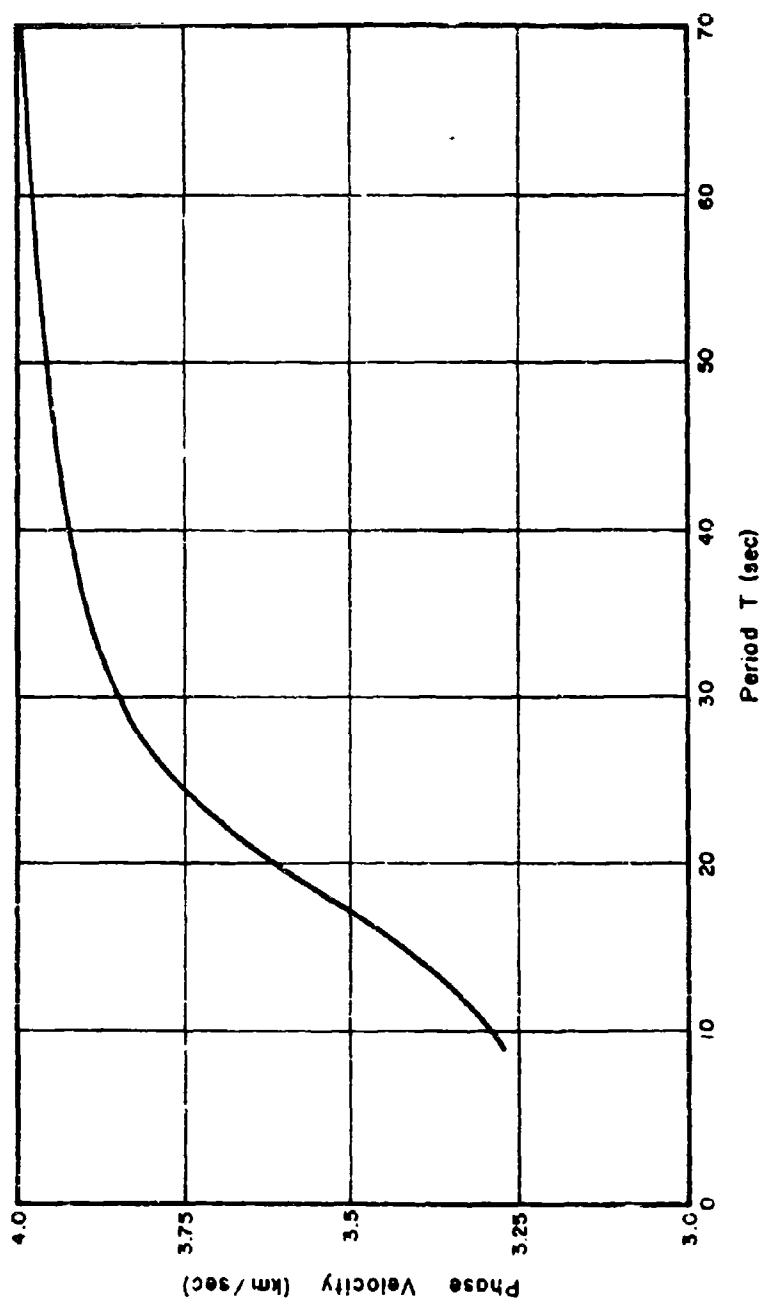
Figure 4. Phase Velocity vs. Period Used for Synthetic Signals

SIGNAL
Δ= 3000 km

Cxy
α =1.0

C
cc=1 0

Δ+100

Cxy
α=0.93

C
cc

Δ+200

Cxy
α=0.97

C
cc=0 97

Figure 5A. Effect of Epicentral Distance Perturbations
on Matched Filter Response.
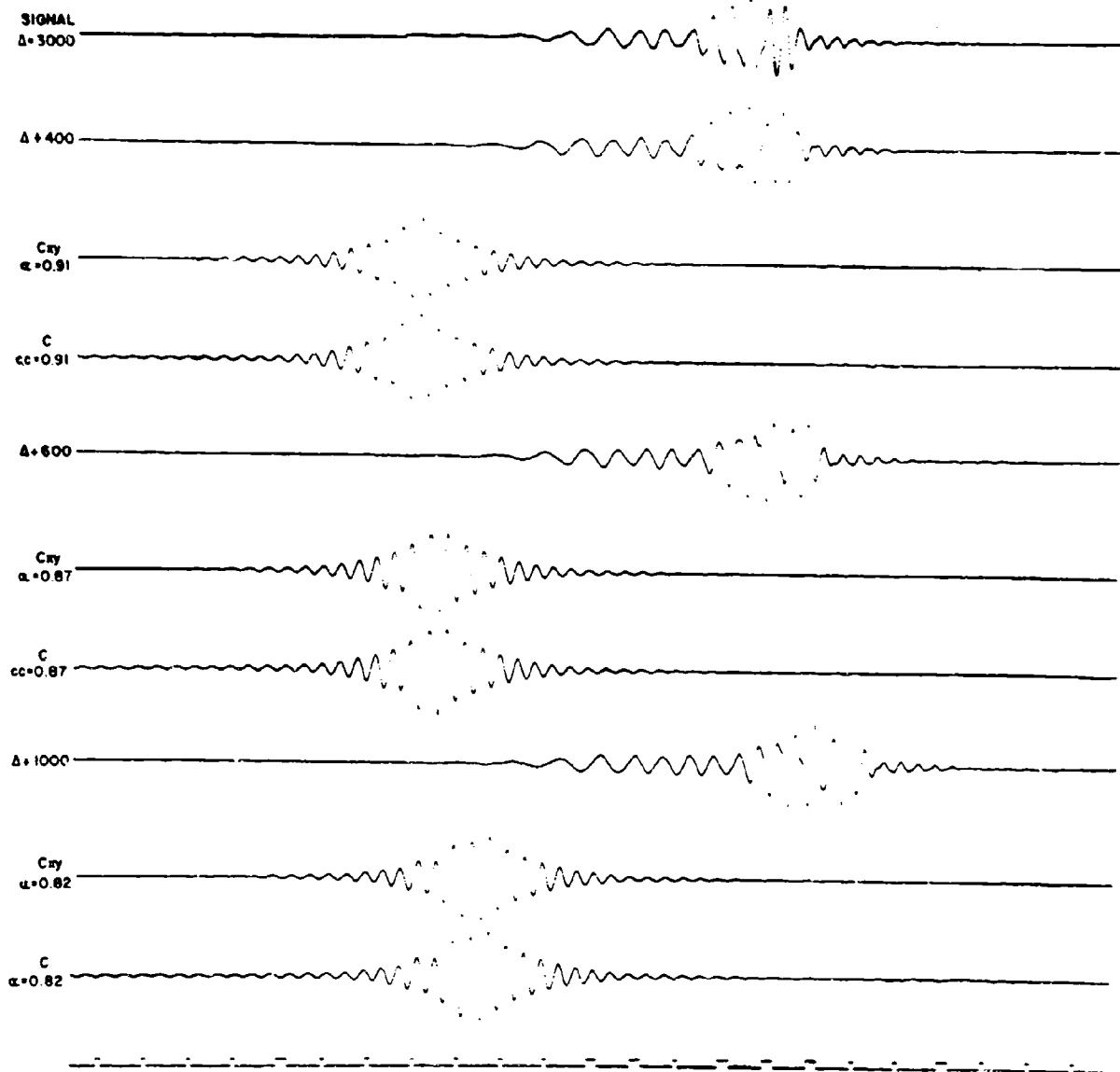
Figure 5B. Effect of Epicentral Distance Perturbations on Matched Filter Response.
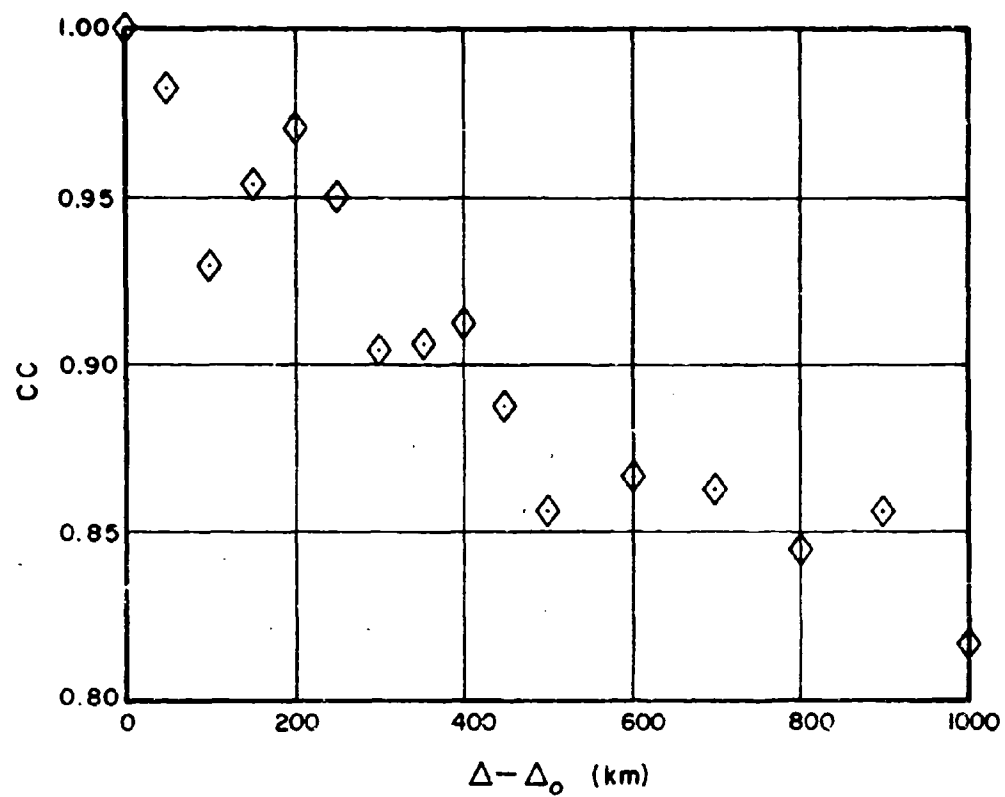
Figure 6. Effect of Differences in Epicentral
Distance on Correlation Coefficient. Dispersion
Curve Used is Shown in Figure 4.
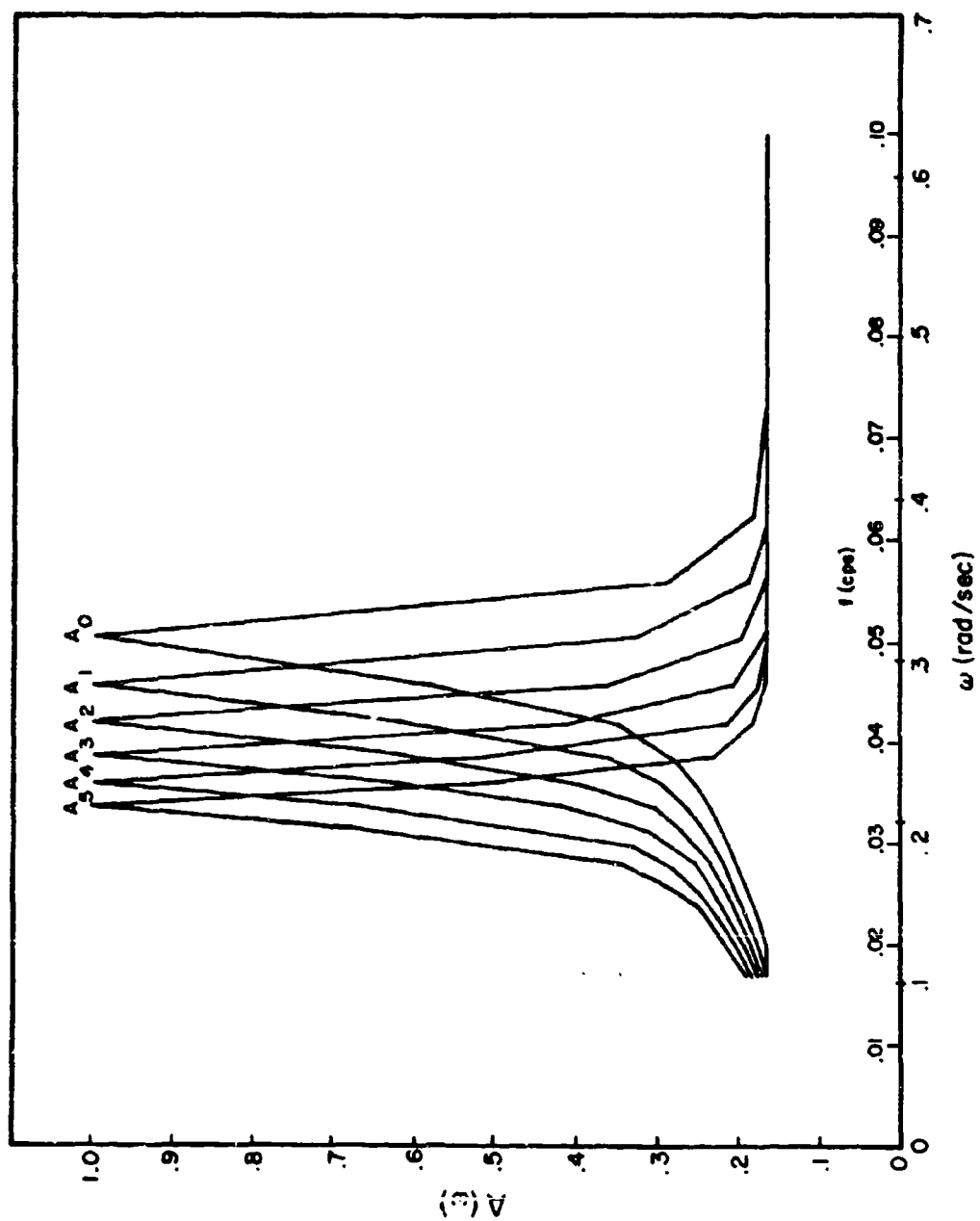
Figure 7. Spectra Used to Test Amplitude Effects on Matched
Filter Response.

SIGNAL
(Ao)
$T_{Pk} = 20$ sec

Cxy
$\alpha = 1.0$

C
$cc = 1.0$

A₁
($T_{Pk} = 22$ sec)

Cxy
$\alpha = 0.835$

C
$cc = 0.869$

A₂
($T_{Pk} = 24$ sec)

Cxy
$\alpha = 0.678$

C
$cc = 0.737$

Figure 8A.   Effect of Amplitude Spectra on Matched Filter
Responue.   The Spectra Ai (f) are Shown in Figure 7.   The
Distance is 3000 km. in Each Case and the Dispersion is
Shown in Figure 4.

SIGNAL
(A_0)
$T_{PK} = 20$ sec

A_3
$(T_{PK} = 26$ sec$)$

C_{xy}
$\alpha = 0.604$

C
$cc = 0.678$

A_4
$T_{PK} = 28$ sec

C_{xy}
$\alpha = 0.575$

C
$cc = 0.645$

A_5
$T_{PK} = 30$ sec

C_{xy}
$\alpha = 0.546$

C
$cc = 0.638$

Figure 8B. Effect of Amplitude Spectra on Matched Filter
Response. The Spectra A_i (f) are Shown in Figure 7. The
Distance is 3000 km. in Each Case and the Dispersion is
Shown in Figure 4.
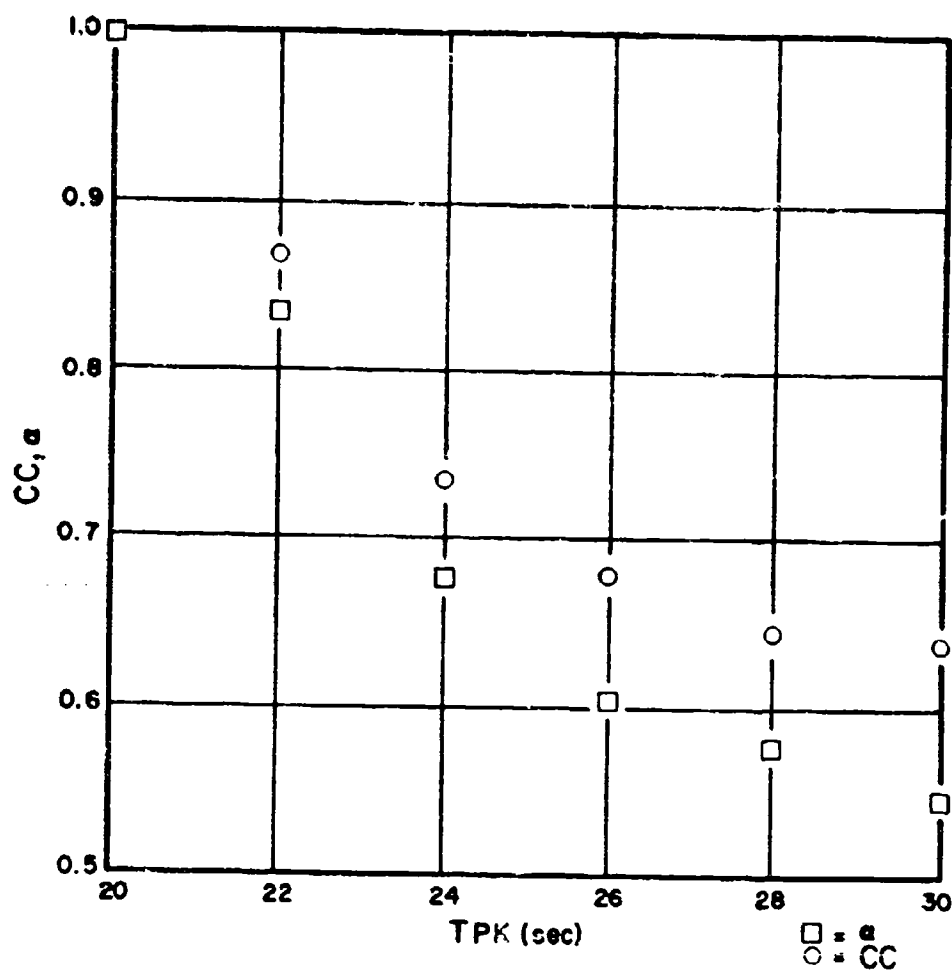
Figure 9. Change in Matched Filter Parameters Due to Shifts in Period of Spectral Peak. (T_o = 20 sec.)
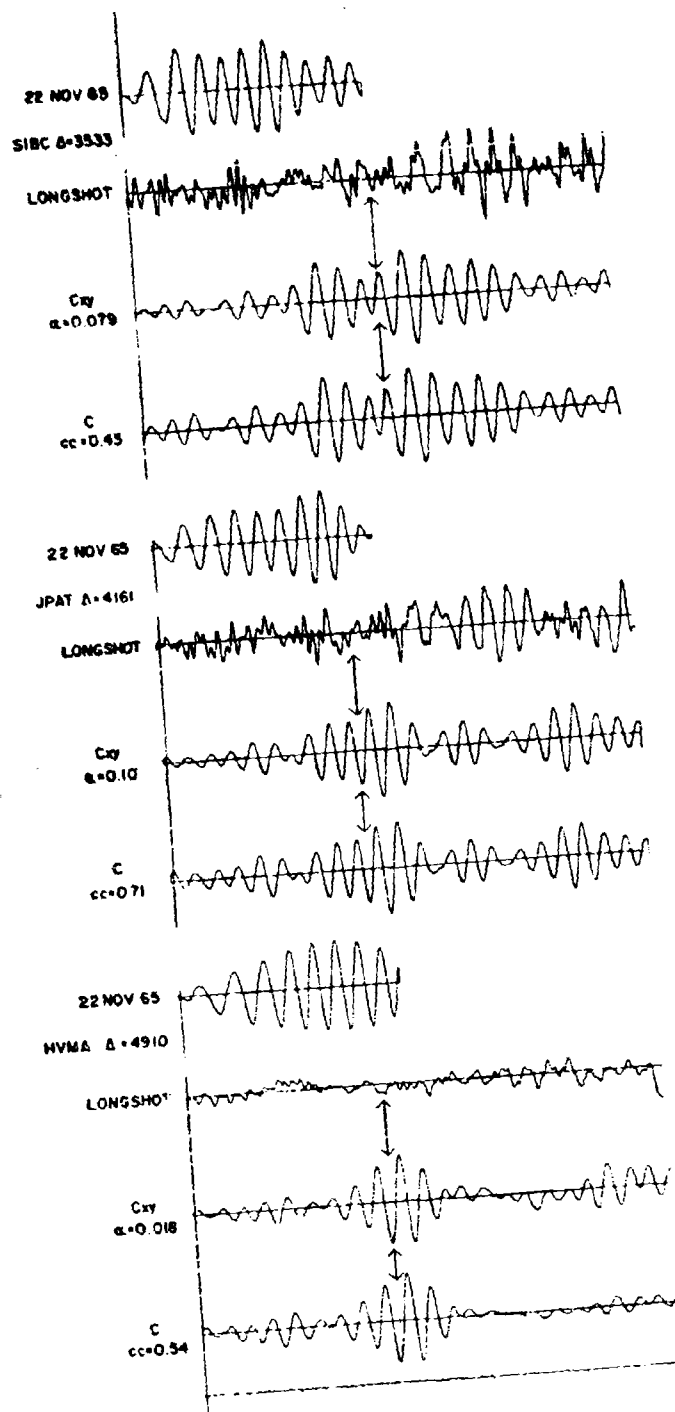
Figure 10A. Matched Filter Analysis of LONGSHOT (m = 5.97) Rayleigh Waves with 22 November 1965 Earthquake (m = 5.9) Rayleigh Waves.
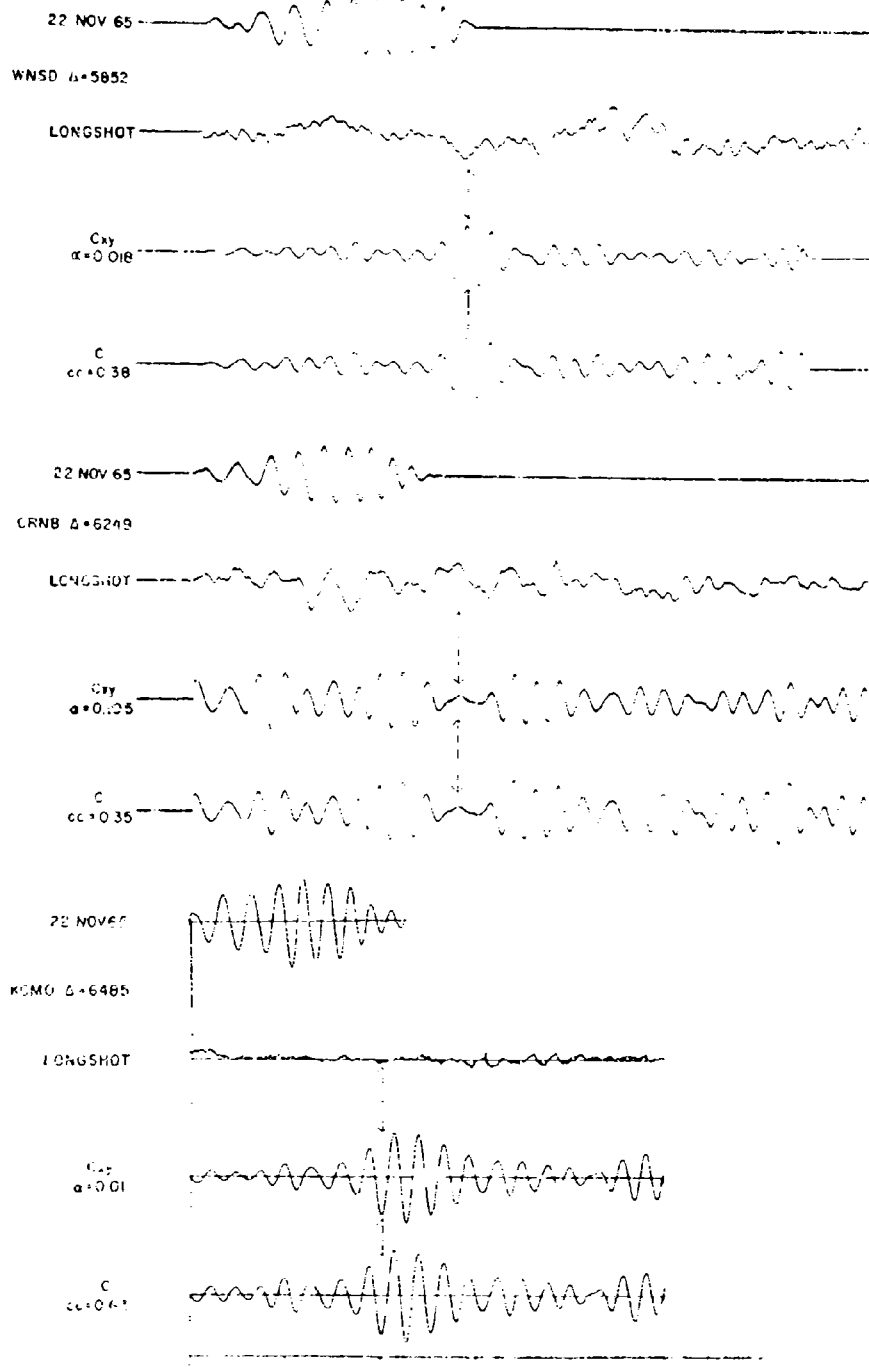
Figure 10B. Matched Filter Analysis of LONGSHOT (m = 5.97)
Rayleigh Waves with 22 November 1965 Earthquake (m = 5.9)
Rayleigh Waves.
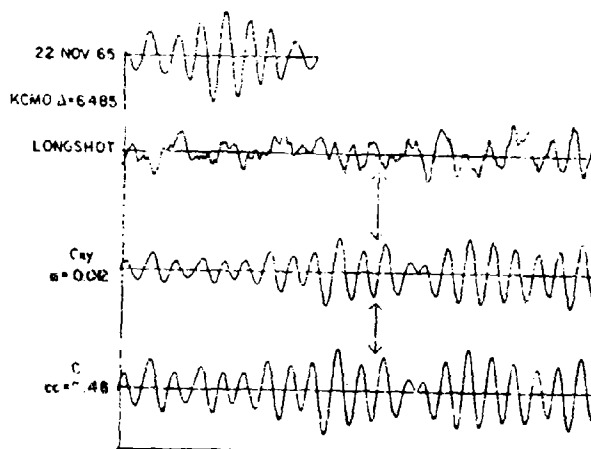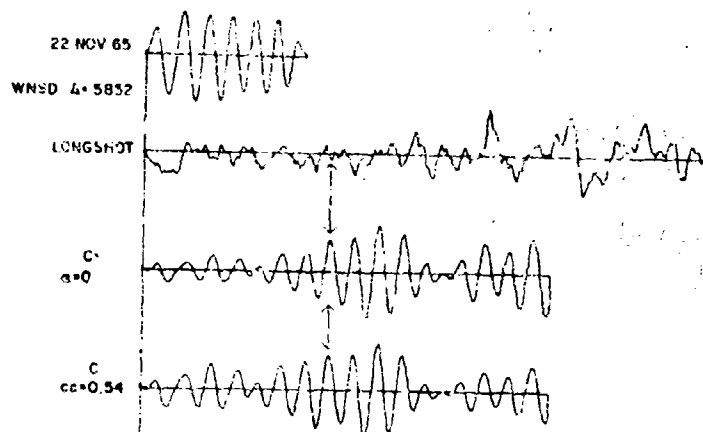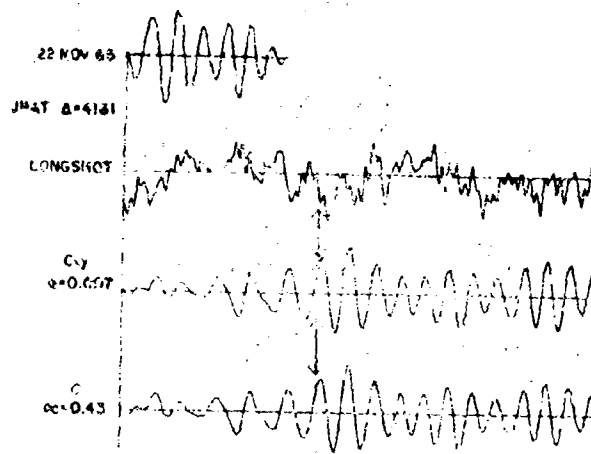
Figure 11. Matched Filter Search for LONGSHOT (m = 5.97) Love Waves with 22 November 1965 Earthquake (m = 5.9) Love Waves.
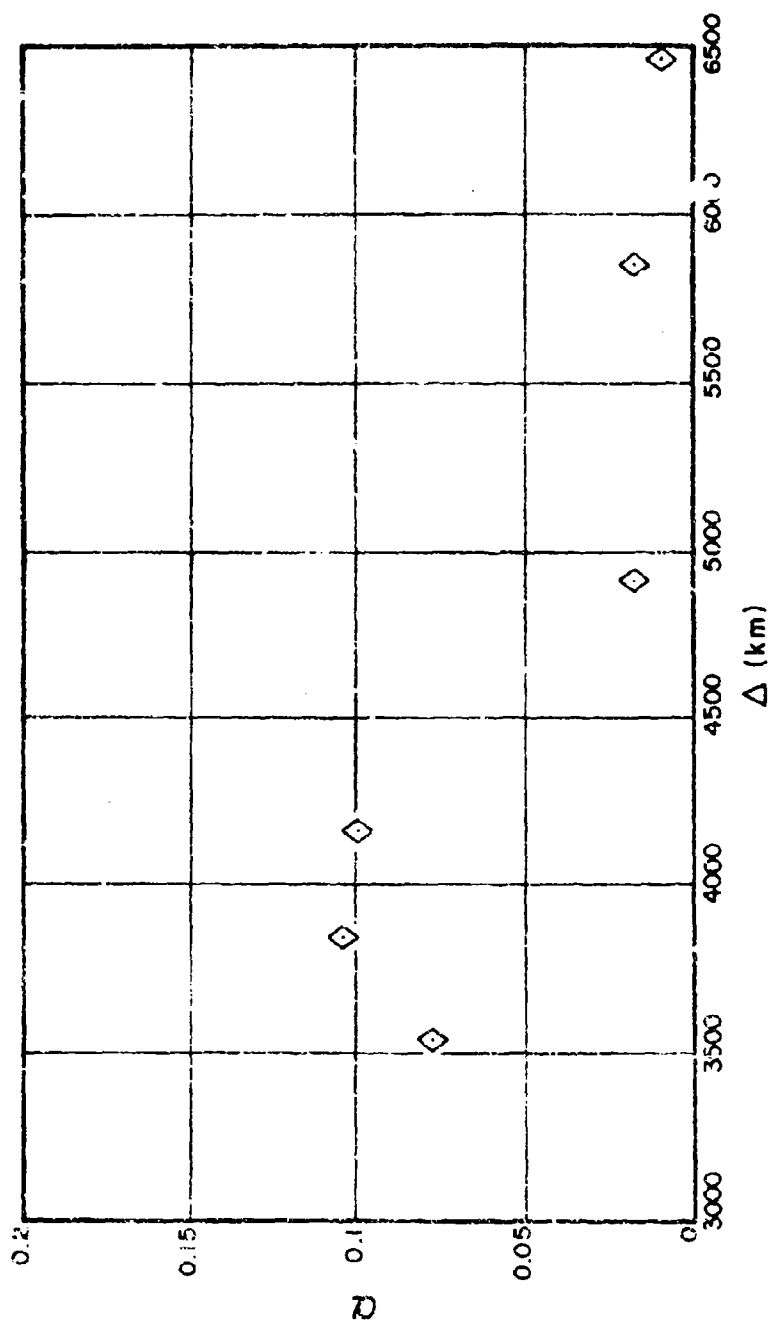
Figure 12. Observed Values of α with Distance for LONGSHOT
Relative to 22 November 1965 Rayleigh Waves. Stations are
Along a Single Azimuth from the Source.

22 NOV 65

SIBC Δ = 3530

25 MAR 66

Cxy

C
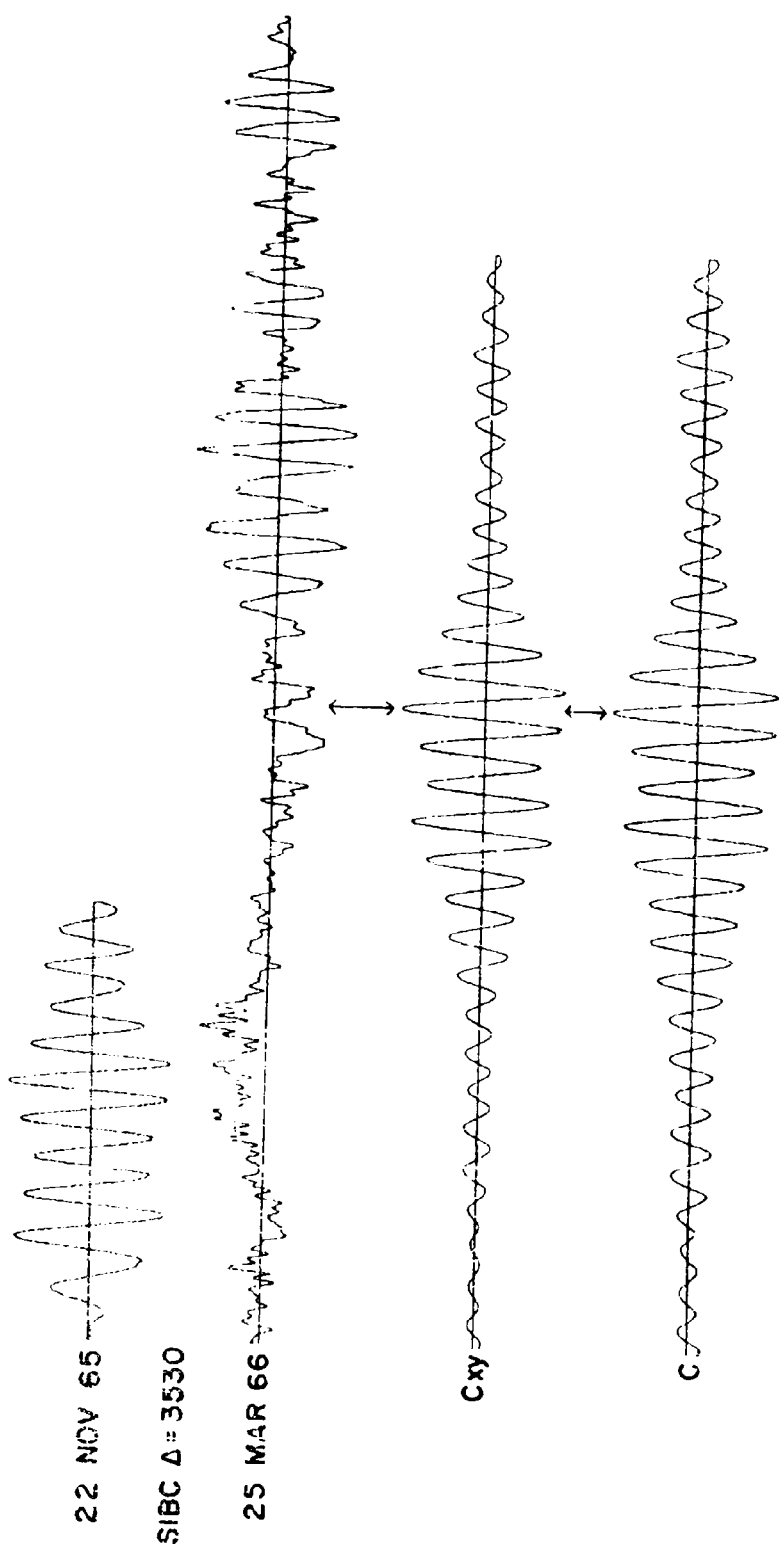
Figure 13. Comparison of Rayleigh Waves from a Magnitude 4.9
Event (25 March 1965) with Those from a Magnitude 5.8 Event
(22 November 1965) Near Andreanof Island.
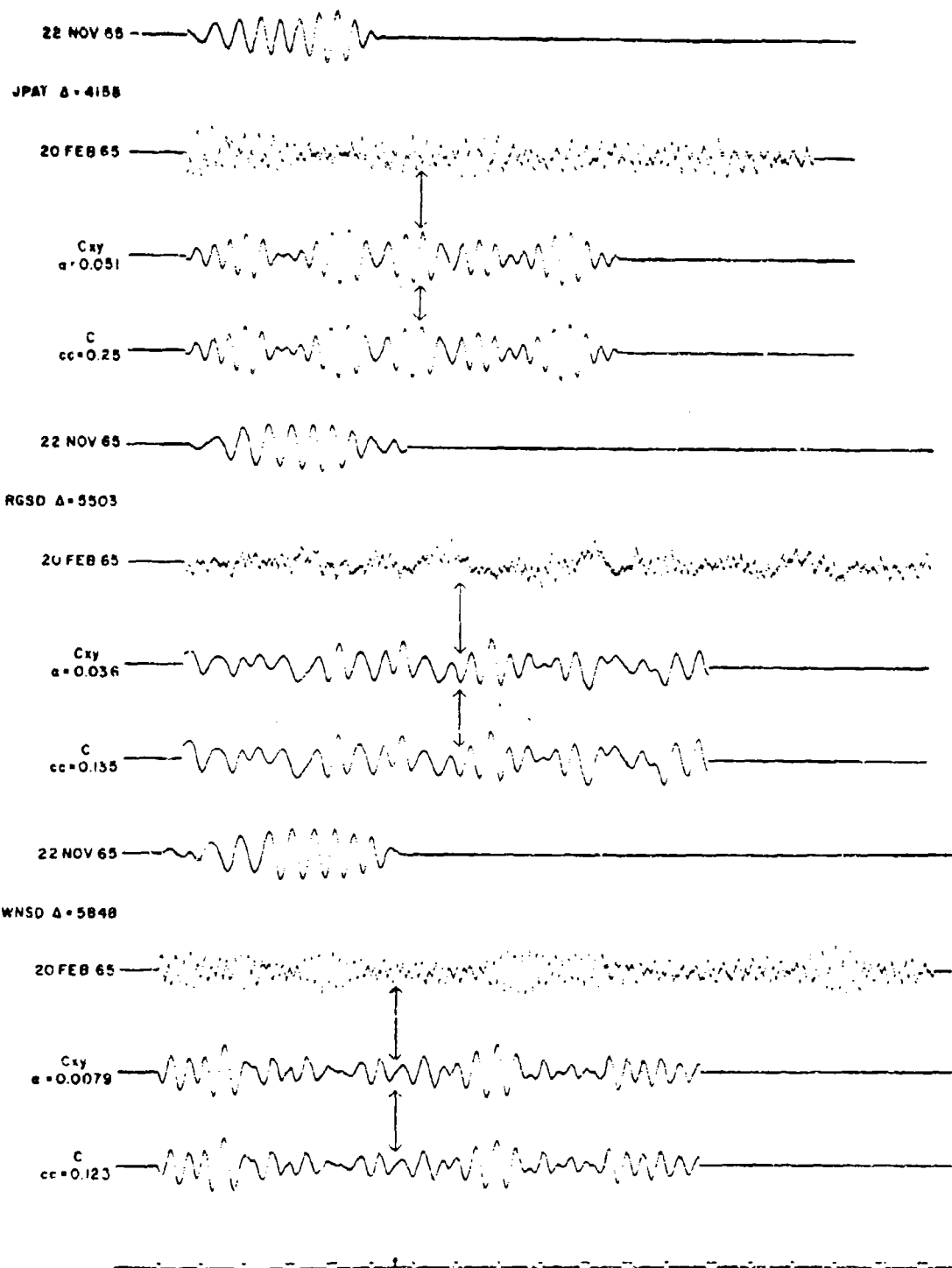
Figure 14A. Search for Rayleigh Waves From a Magnitude 4.0 Event at Depth 48 km. Using 22 November 1965 Magnitude 5.9 Event.

22 NOV 65

CRNB Δ=6244

20 FEB 66

Cxy
α=0.0093

C
cc=0.022

22 NOV 65

KCMO Δ=6480

20 FEB 66

Cxy
α=0.0066

C
cc=0.10

22 NOV 65

ENMO Δ=6928

20 FEB 66

Cxy
α=0.0098

C
cc=0.15
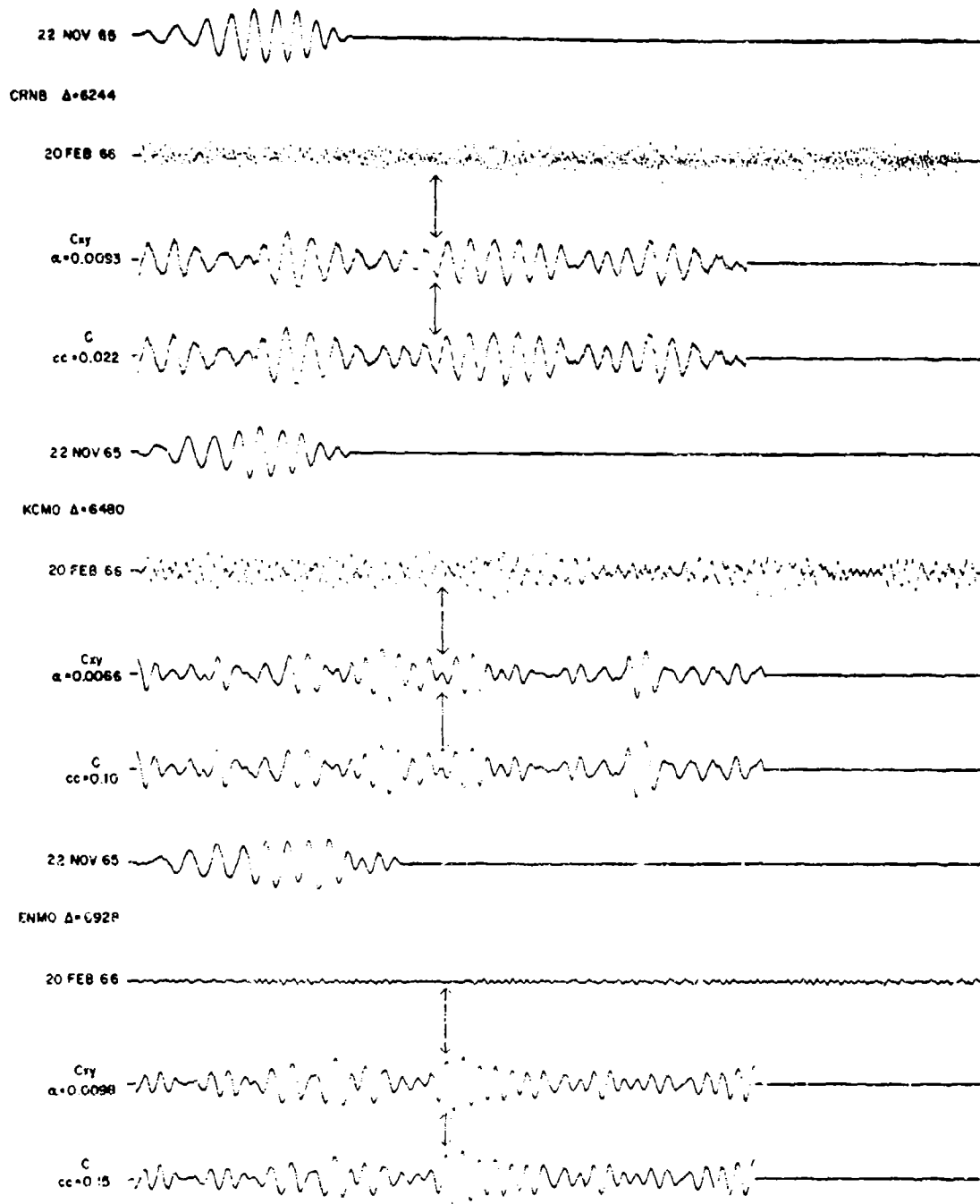
Figure 14B. Search for Rayleigh Waves From a Magnitude
4.0 Event at Depth 48 km, Using 22 November 1965 Magni-
tude 5.9 Event.

Figure 15A. Matched Filter Comparison of Rayleigh Waves From a Magnitude 5.8 Event (29 January 1965) with Those from a Magnitude 5.3 Event (20 April 1965) in Kamchatka.

Figure 15B. Matched Filter Comparison of Rayleigh Waves From a Magnitude 5.8 Event (29 January 1965) with Those from a Magnitude 5.3 Event (20 April 1965) in Kamchatka.

29 JAN 65

HNME Δ=7914

20 APR 65

Cxy
α=0.14

C
cc=0.25

29 JAN 65

BRPA Δ=8061

20 APR 65

Cxy
α=0.098

C
cc=0.28

29 JAN 65

Δ=8109

20 APR 65

Cxy
α=0.0073

C
cc=0.009

Figure 15C. Matched Filter Comparison of Rayleigh Waves From
a Magnitude 5.5 Event (29 January 1965) with Those from a Mag-
nitude 5.3 Event (20 April 1965) in Kamchatka.
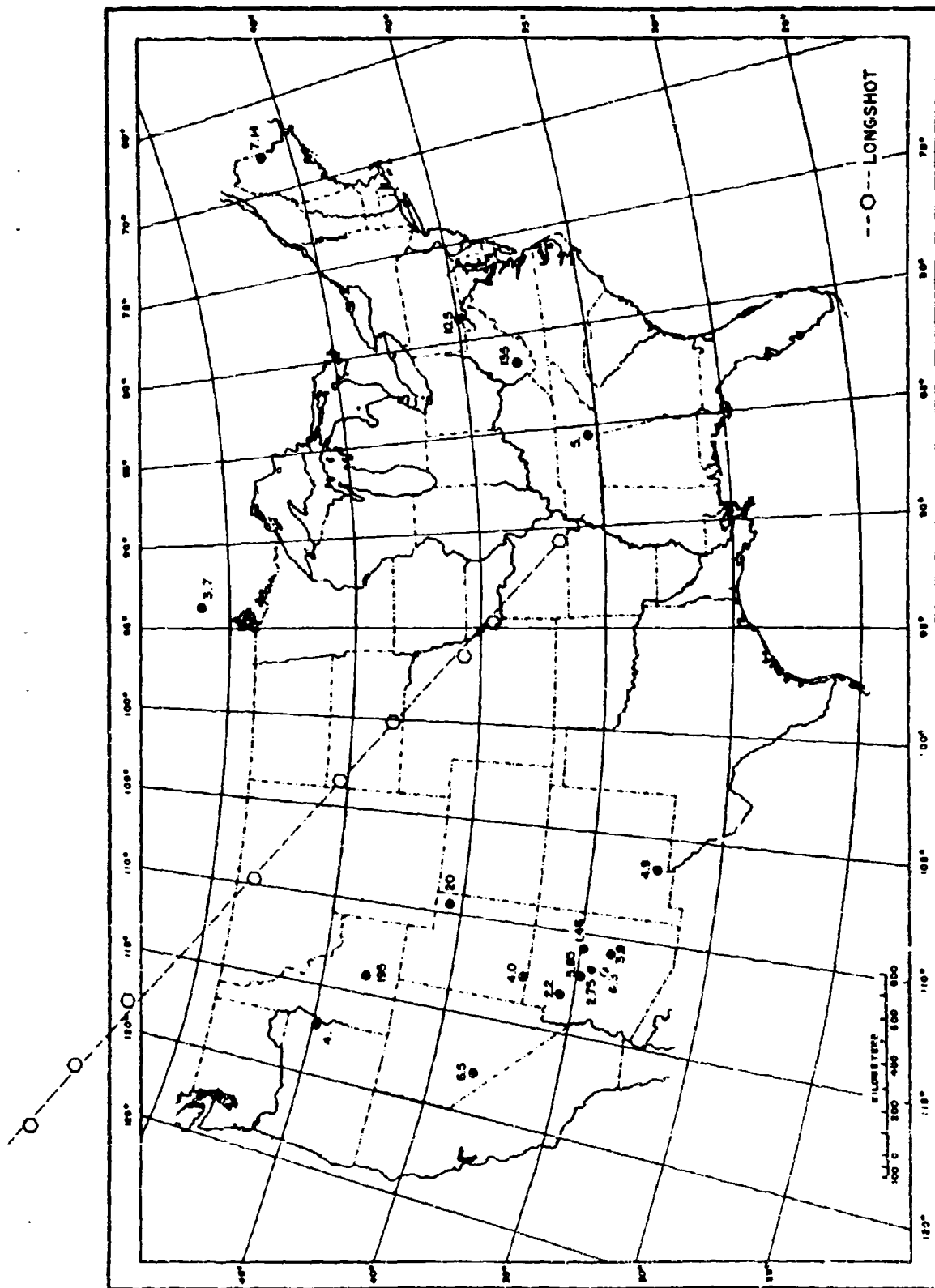
Figure 16. Observed Relative Excitation (α) of Rayleigh Waves Between a Magnitude 5.8 Event (29 January 1965) and a Magnitude 5.3 Event (20 April 1965) Located in Kamchatka. A LONGSHOT Profile is Also Shown.
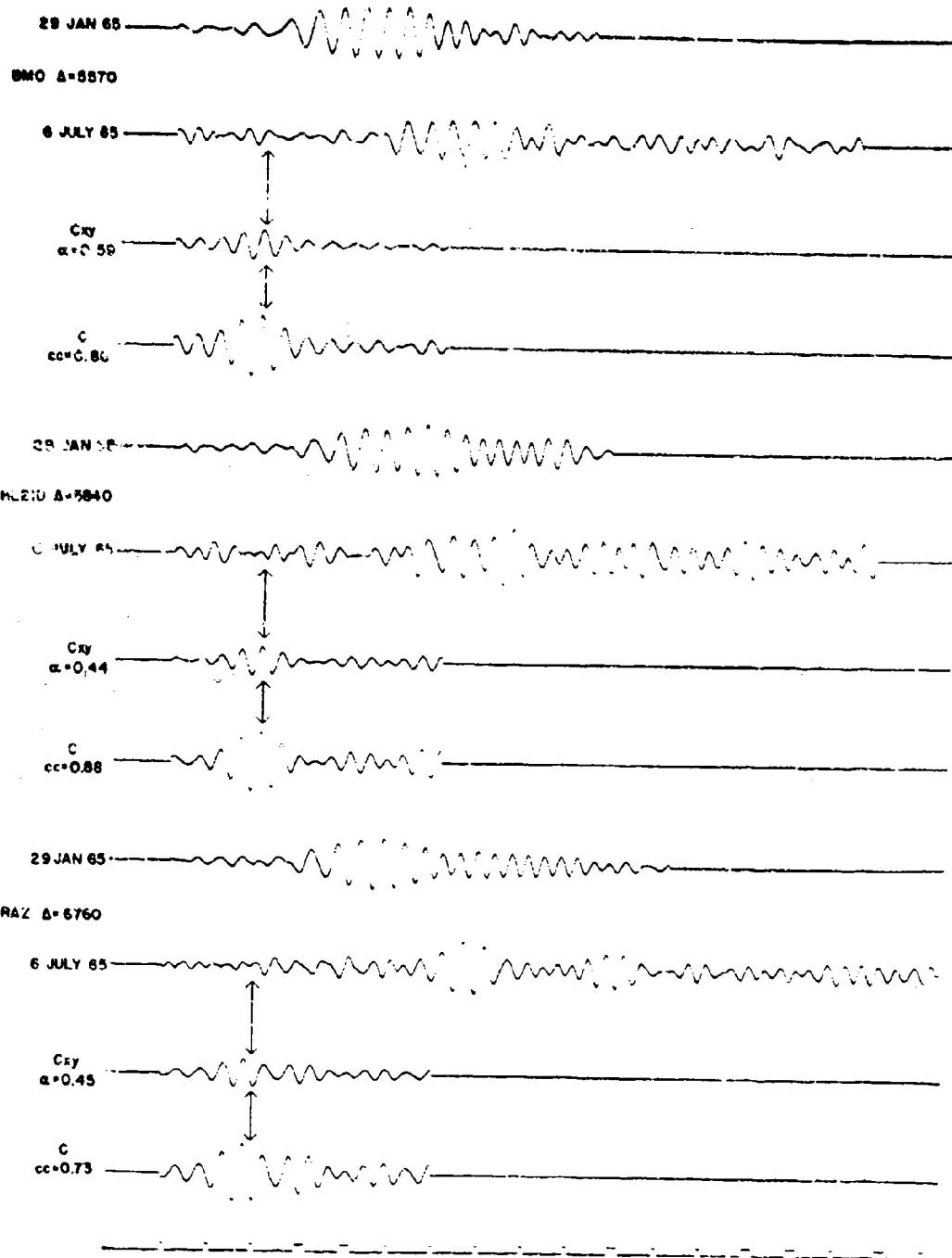
Figure 17A. Matched Filter Comparison of Rayleigh Waves From a Magnitude 5.8 Event (29 January 1965) With Those From a Magnitude 5.1 Event (6 July 1965) in Kamchatka.
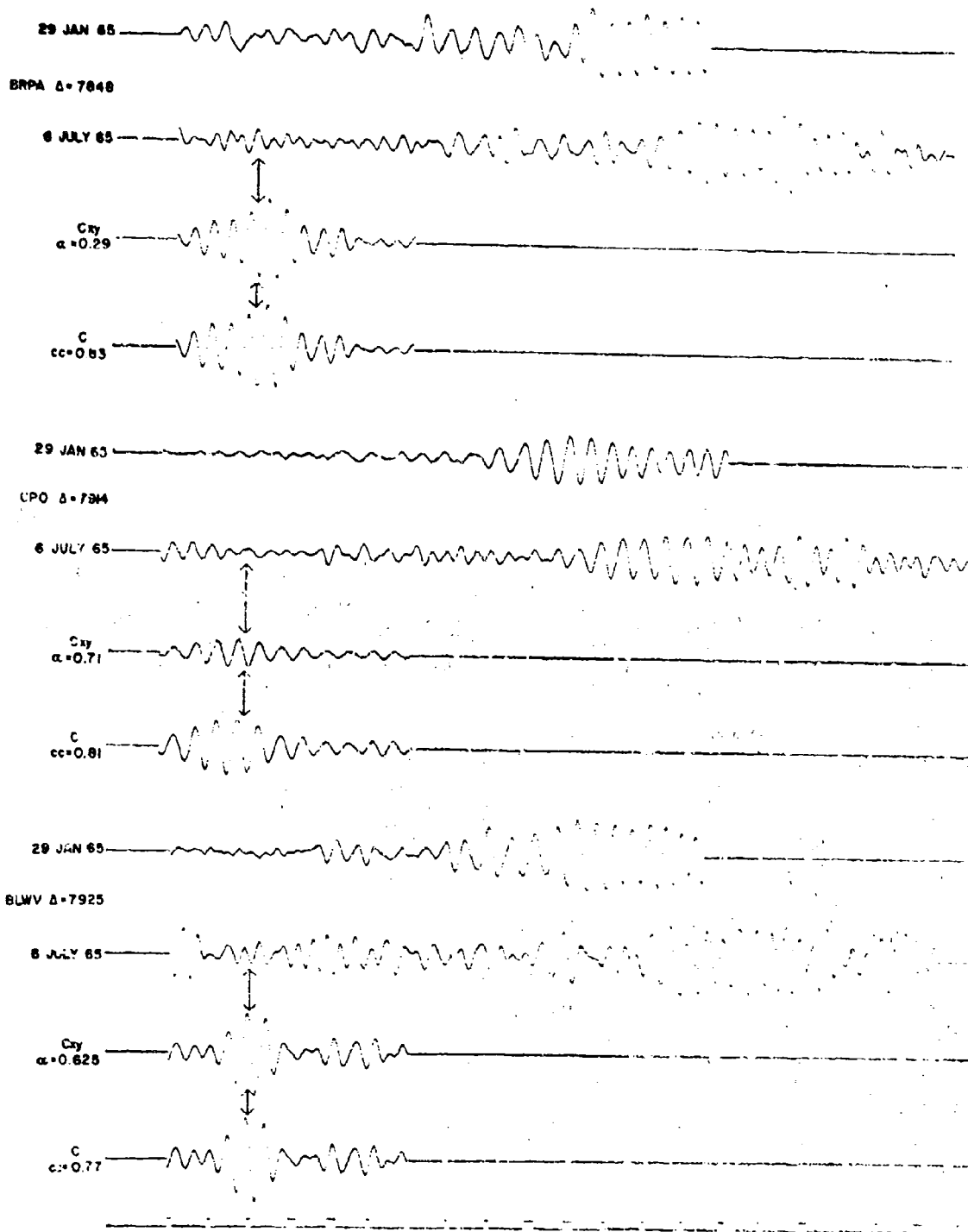
Figure 17B. Matched Filter Comparison of Rayleigh Waves From
a Magnitude 5.8 Event (29 January 1965) With Those From a
Magnitude 5.1 Event (6 July 1965) in Kamchatka.

29 JAN 65

HKON Δ=6183

14 FEB 65

Cxy
α=0.088

C
cc=0.51

29 JAN 55

HRAZ Δ=6560

14 FEB 65

Cxy
α=0.043

C
cc=0.35

29 JAN 65

WMO Δ=7282

14 FEB 65

Cxy
α=0.098

C
cc=0.24
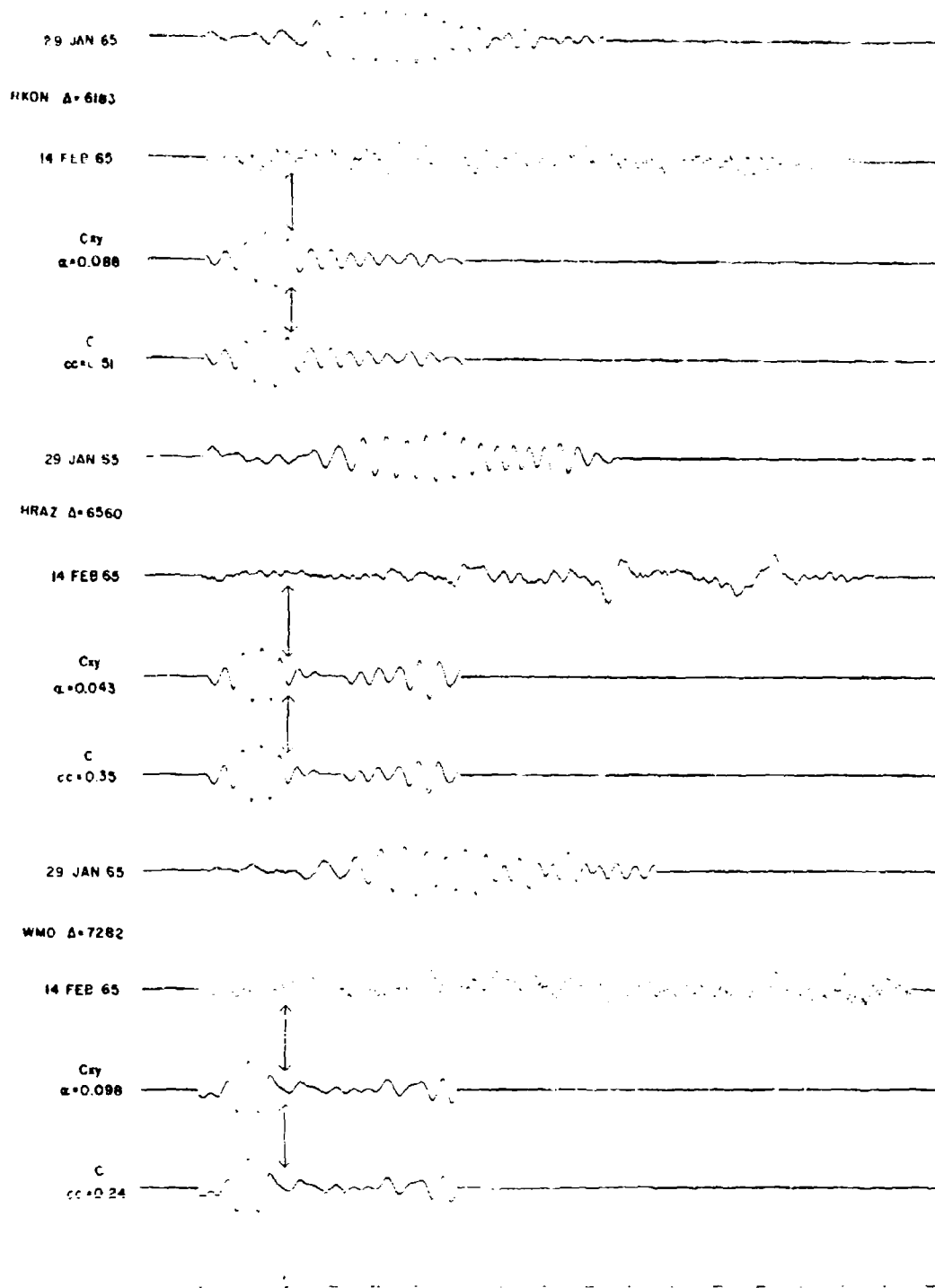
Figure 18A. Matched Filter Comparison of Rayleigh Waves
From a Magnitude 5.9 Event (29 January 1965) With Those
From a Magnitude 5.0 Event (14 February 1965) in Kamchatka.

29 JAN 65

BMO Δ·5372

14 FEB 65

Cxy
α·0.062

C
cc·0.60

29 JAN 65

HL2ID Δ·5639

14 FEB 65

Cxy
α·0.056

C
cc·0.51

29 JAN 65

U8O Δ·6172

14 FEB 65

Cxy
α·0.046

C
cc·0.38

Figure 18B. Matched Filter Comparison of Rayleigh Waves
From a Magnitud 5.8 Event (29 January 1965) With Those
From a Magnitude 5.0 Event (14 February 1965) in Kamchatka.
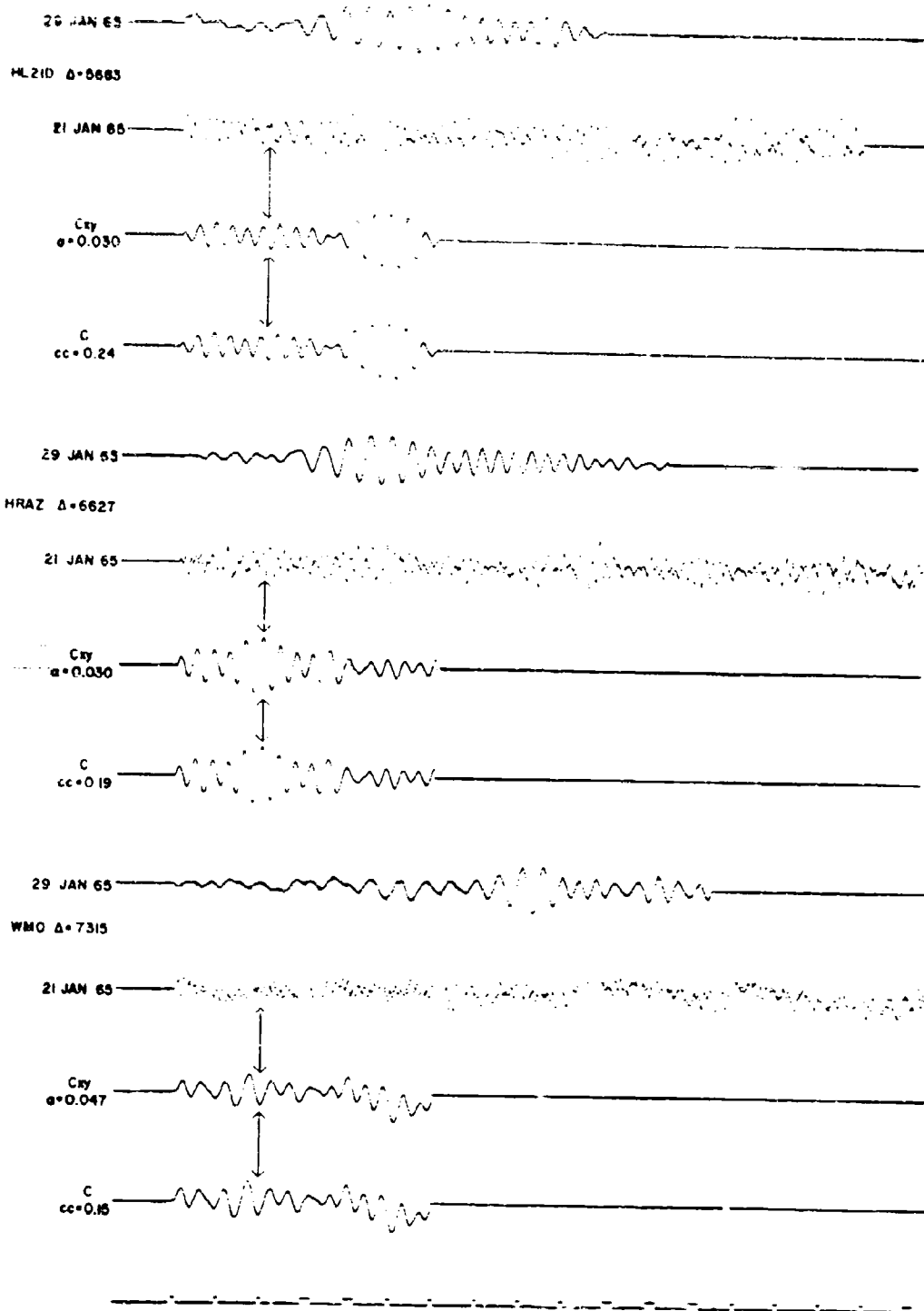
Figure 19. Search for Rayleigh Waves From a Magnitude 4.4
Event at Depth 119 km. Using the Magnitude 5.8 Event of 29
January 1965.

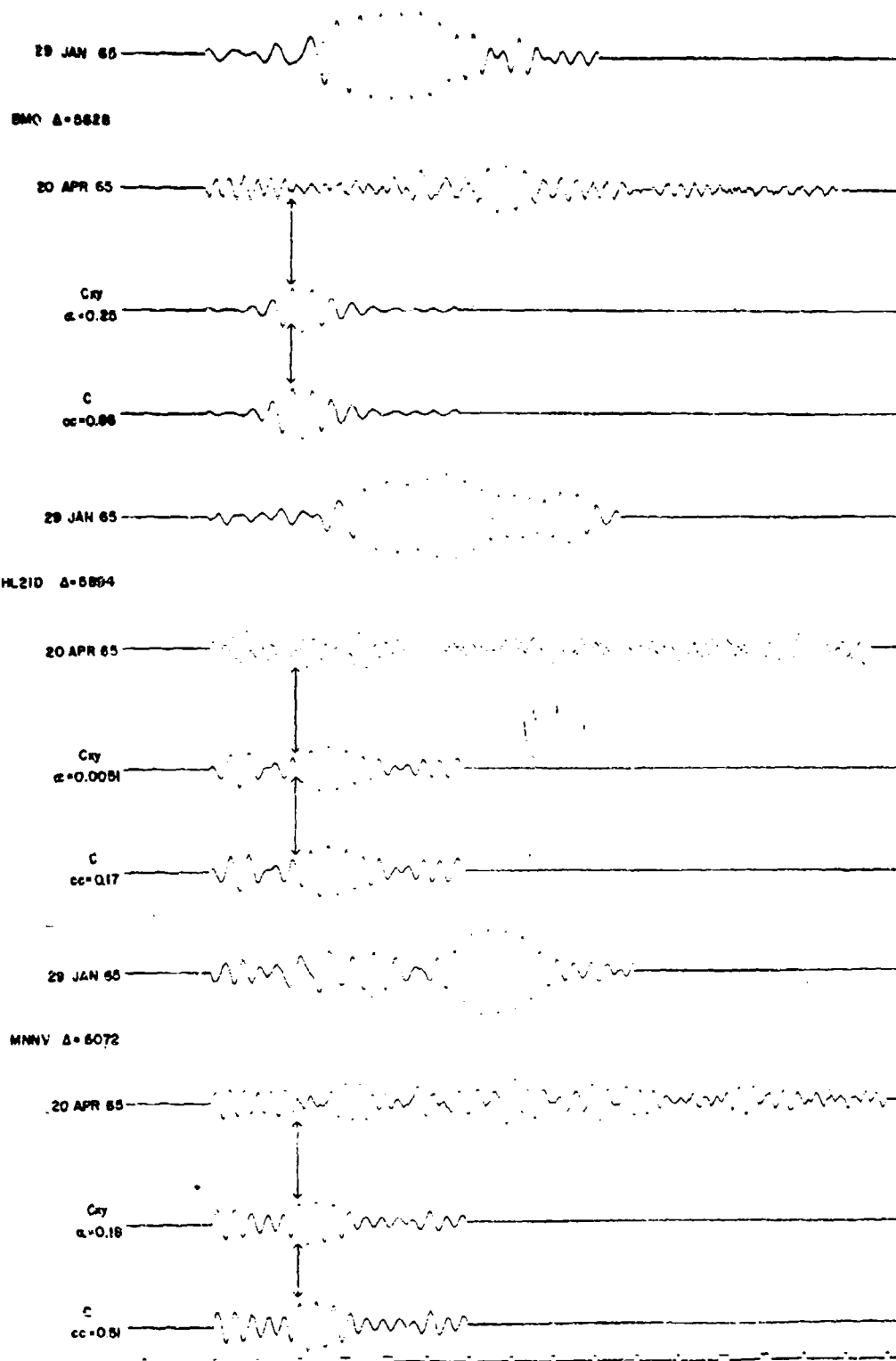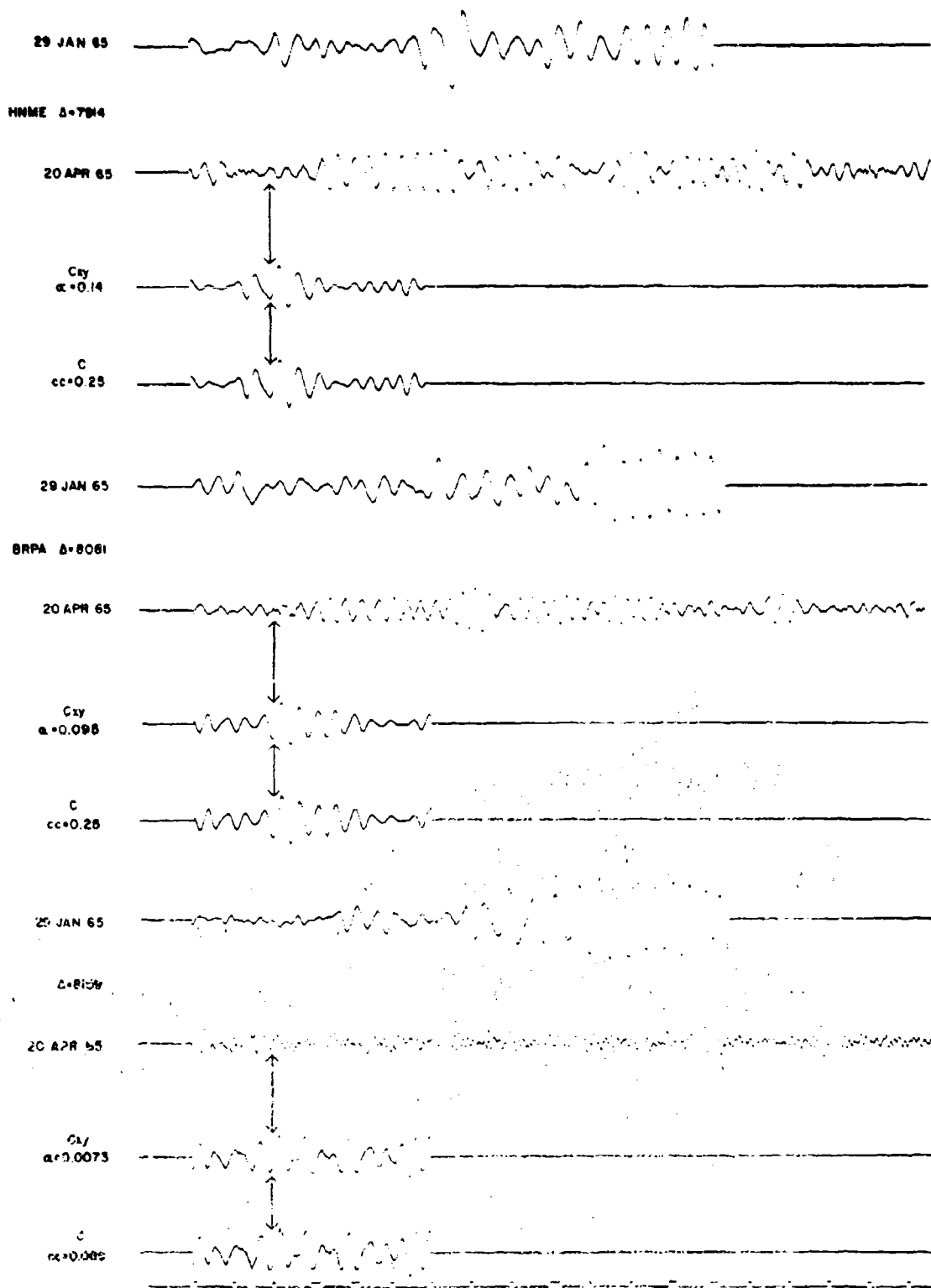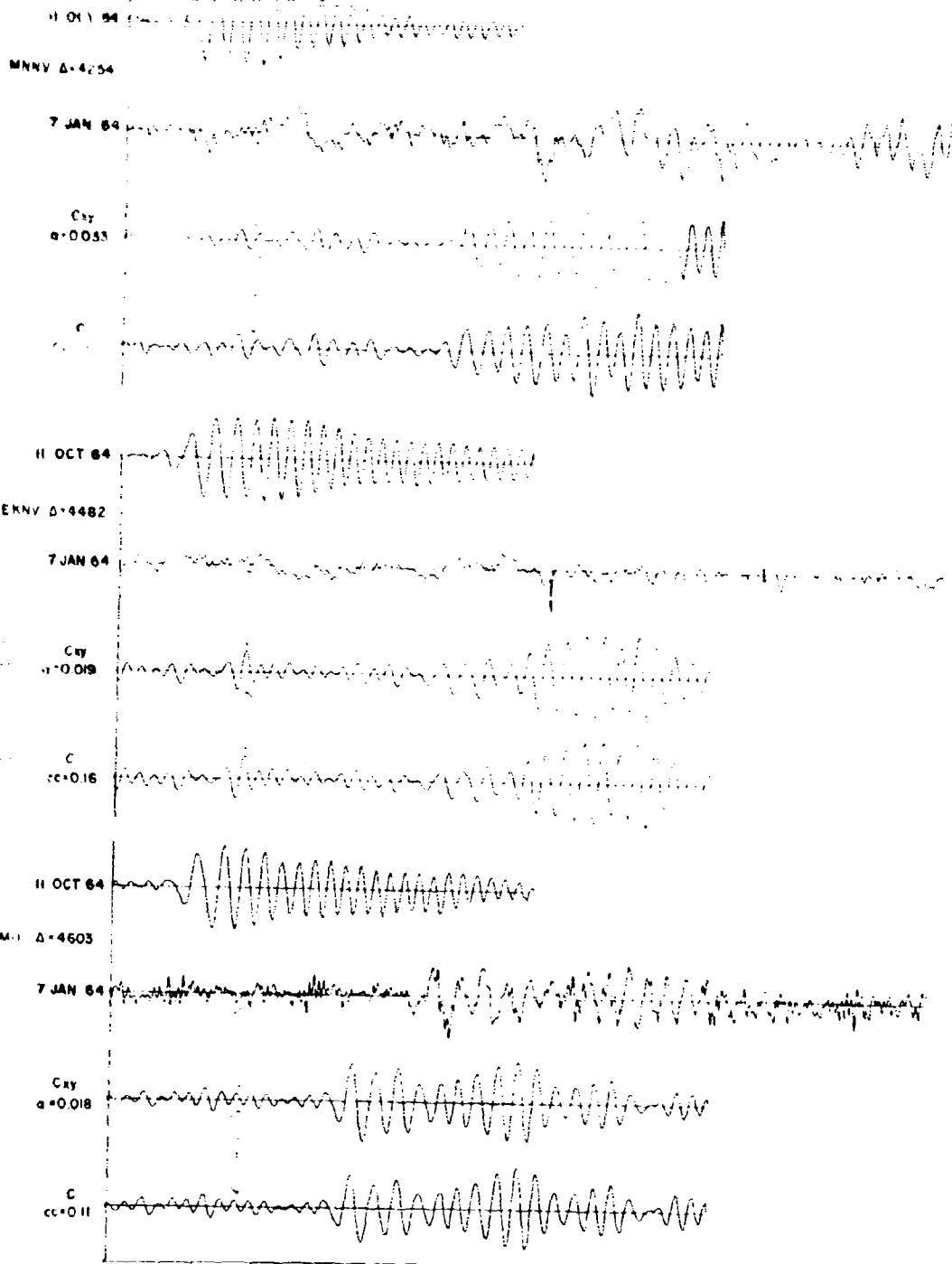Figure 20A. Search for Rayleigh Waves From a Magnitude 4.4
Event (7 January 1964) Using Those From a Magnitude 5.3
Event (11 October 1964) in Hawaii. The Surface Wave Train
Arriving Later on These Records is From a Magnitude 5.0
in New Guinea.
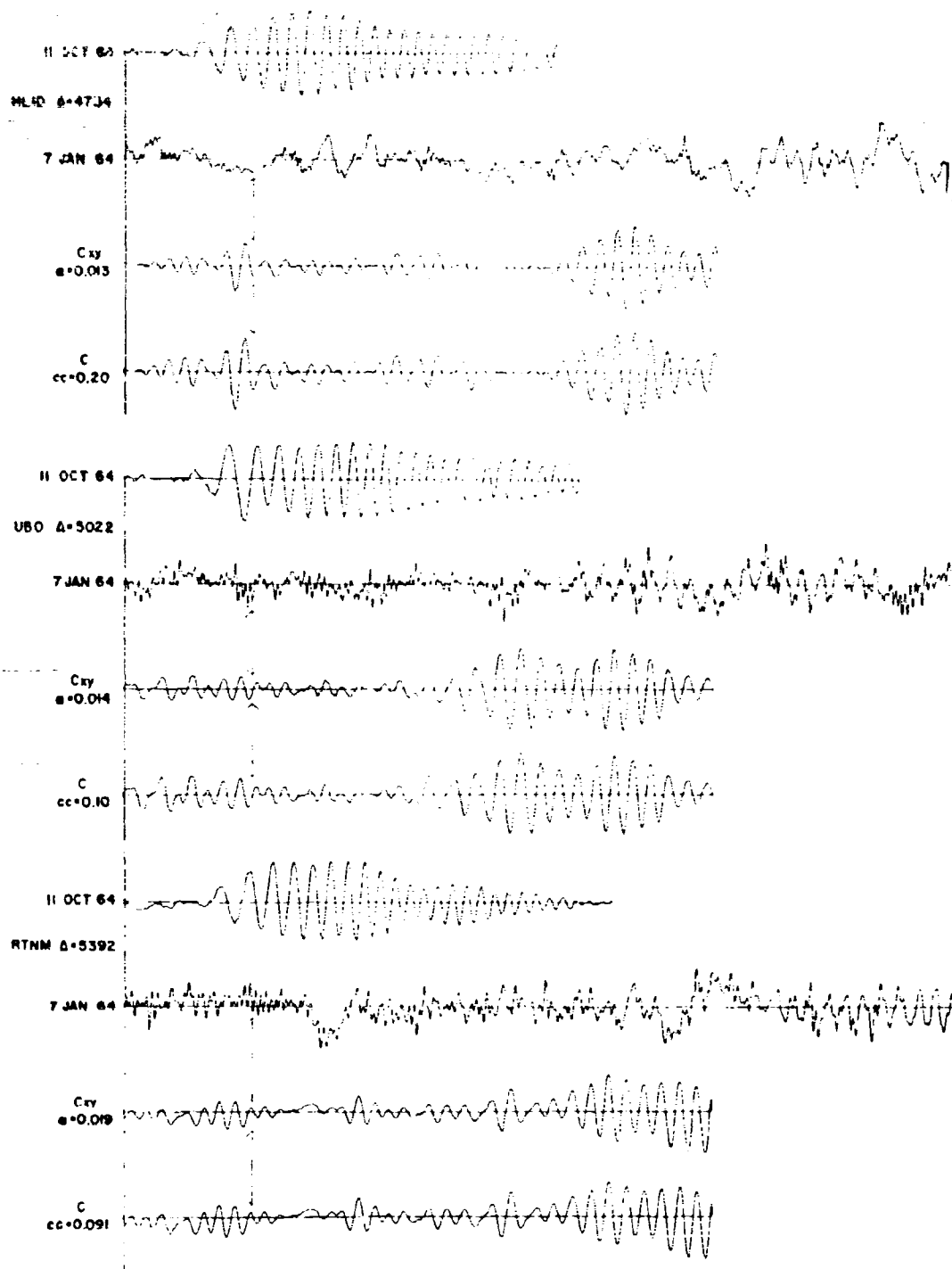
Figure 20B. Search for Rayleigh Waves From a Magnitude 4.4 Event (7 January 1964) Using Those From a Magnitude 5.3 Event (11 October 1964) in Hawaii. The Surface Wave Train Arriving Later on These Records is From a Magnitude 5.0 in New Guinea.
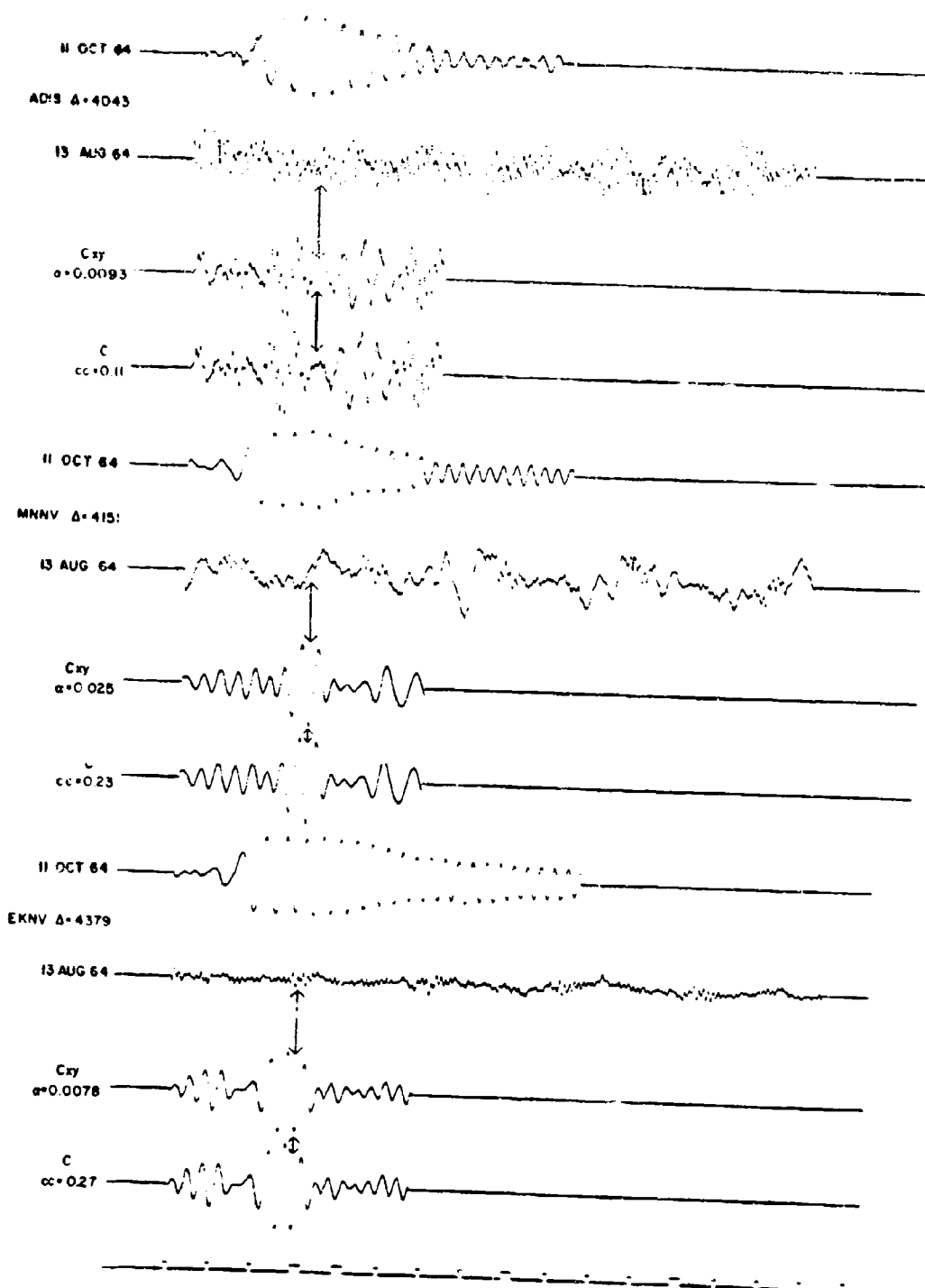
Figure 21A. Search for Rayleigh Waves From a Magnitude 4.1
Event (13 August 1964) Using Those From a Magnitude 5.3
Event (11 October 1964) in Hawaii.
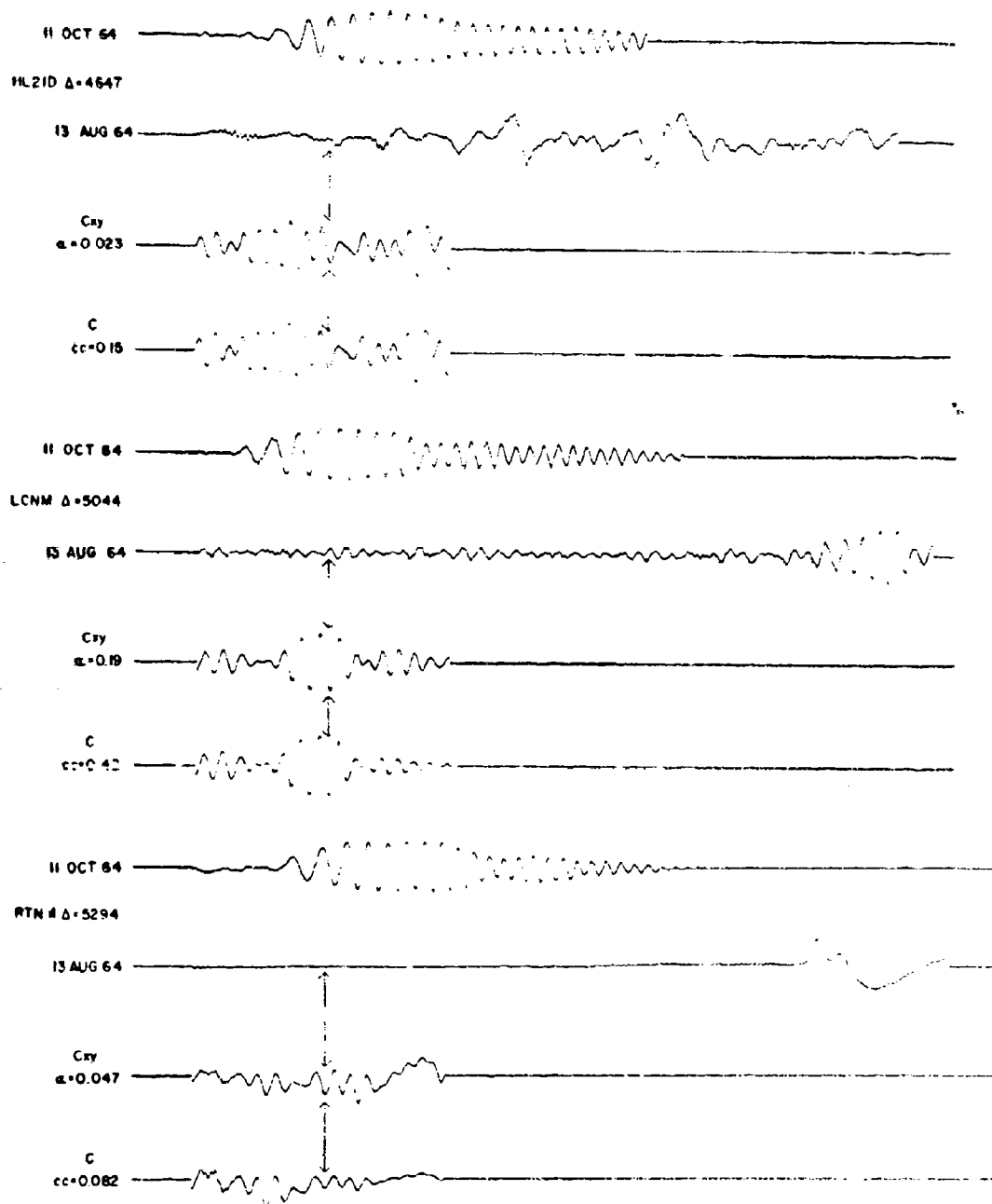
Figure 21B. Search for Rayleigh Waves From a Magnitude 4.1
Event (13 August 1964) Using Those From a Magnitude 5.3
Event (11 October 1964) in Hawaii.

Date	Area	Origin Time	Latitude	Longitude	Magnitude	Depth
25 Mar 66	Andreanof Is.	12:54:55.7	51.5N	179.6E	4.9	33
20 Feb 66	Rat Is.	8:27:58.0	51.1 N	179.5 E	4.0	48
22 Nov 65	Andreanof Is.	20:25:30.4	51.3 N	179.8 W	5.9*	40
29 Oct 65	Amchitka Is.	21:00:00.1	51 4 N	179.2 E	5.97	0(Longshot)
6 Jul 65	Kamchatka	4:58:55.7	55.1 N	162.1 E	5.1	33
20 Apr 65	Kamchatka	6:50:17.6	54.6 N	161.4 E	5.3	33
14 Feb 65	Komandorsky	17:01:13.9	55.1 N	165.6 E	5.0	20
29 Jan 65	Kamchatka	9:35:25.7	54.8 N	161.7 E	5.8*	33
21 Jan 65	Kamchatka	16:36:46.2	56.2 N	163.1 E	4.4	119
11 Oct 64	Hawaii	10:06:44.9	19.1 N	156.6 W	5.3*	33
13 Aug 64	Hawaii	16:27:35.4	19.5 N	155.4 W	4.1	11
7 Jan 64	Hawaii	11:06:21.0	18.6 N	155.9 W	4.4	33

*Used as filter for others in group

Table I   Epicenter Information (from USC&GS)

INDIRECT METHOD FOR OBTAINING SPECTRUM OF SMALL EVENTS

From the analysis in the text, we have

$$\hat{a}(\tau) \sum_{t} y^2(t) = \sum_{t} x(t+\tau) y(t) \qquad (\text{I-1})$$

The frequency-domain equivalent of (I-1) is

$$\hat{a}(\tau) \int_0^\infty Y(\omega) Y^*(\omega) d\omega = \int_0^\infty X(\omega) Y^*(\omega) e^{i\omega\tau} d\omega \qquad (\text{I-2})$$

where $Y(\omega)$ and $X(\omega)$ are the Fourier transforms of $y(t)$ and $X(t)$ respectively. Without losing generality, τ can be taken as zero, since it is arbitrary in the analysis.

If this is done, we have

$$\hat{a} \int_0^\infty Y(\omega) Y^*(\omega) d\omega = \int_0^\infty X(\omega) Y^*(\omega) d\omega \qquad (\text{I-3})$$

We know in addition that in propagating over a distance Δ from Δ_0, the spectral amplitude is reduced by a factor

$$\left[\frac{\sin \Delta_0}{\sin(\Delta + \Delta_0)} \right]^{\frac{1}{2}} exp\left[-2g(\omega)\Delta \right]$$

where $2g(\omega) \approx \omega/[Q\,U(\omega)]$, Q is the quality factor characteristic of the attenuation due to anelasticity, ω is radian frequency, and $U(\omega)$ is the group velocity. We see that the exponential factor describes the amplitude decay due to departure from perfect elasticity,

and the term in brackets describes the effect of geometrical spreading.

We see that if $\hat{a}$ is determined at several distances along a given azimuth from the source, we can generalize (I-3) to

$$\hat{a}(\Delta) \int_0^{\infty} \Upsilon^2(\omega, \Delta_0)\, e^{-2g(\omega)\Delta}\, d\omega$$

$$= \int_0^{\infty} \chi(\omega, \Delta_0)\, \Upsilon^*(\omega, \Delta_0)\, e^{-2g(\omega)\Delta}\, d\omega \tag{I-4}$$

where the reference distance Δ_0 corresponds to $\Delta = 0$. The propagation phase factors cancel, since the transmission path (hence the dispersion) is identical for the two events. The geometrical spreading factor also cancels on both sides of (I-4).

If we now make the approximation

$$2g(\omega) \approx c\omega \tag{I-5}$$

where $\qquad c = (QU)^{-1}$

is assumed to be constant, we can write (I-4) in the form

$$\hat{a}(\Delta)\, c^{-1} \int_0^{\infty} \Upsilon^2(\omega'/c, \Delta_0)\, e^{-\omega'\Delta}\, d\omega'$$

$$= c^{-1} \int_0^{\infty} \chi(\omega'/c, \Delta_0)\, \Upsilon^*(\omega'/c, \Delta_0)\, e^{-\omega'\Delta}\, d\omega' \tag{I-6}$$

where $\omega' = c\omega$.

- 2 -

The integrals in this expression are now in the form of r ~~~~ace transform with respect to Δ . Carrying out the inversion of both sides of (I-6) and changing the order of integration on the left, we have

$$c^{-} \int_0^\infty Y^2(\omega'/c, \Delta_o) \int_{\beta-i\infty}^{\beta+i\infty} \hat{a}(\Delta)\, e^{-\omega'\Delta}\, e^{s\Delta}\, d\Delta\, d\omega'$$

$$= c^{-1}\, X(s/c, \Delta_o)\, Y^*(s/c, \Delta_o) \tag{I-7}$$

or

$$c^{-1} \int_0^\infty Y^2(\omega'/c, \Delta_o)\, \bar{a}(s-\omega')\, d\omega' = c^{-1} X(s/c, \Delta_o)\, Y^*(s/c, \Delta_o) \tag{I-8}$$

That is, the left-hand side is the convolution of $Y^2(s/c)$ with $\bar{a}(s)$, the inverse transform of $\hat{a}(\Delta)$. From (I-8) we can find $X(s/c, \Delta_o)$ directly by carrying out this convolution and dividing the result by $Y^*(s/c, \Delta_o)$. Equivalently, if we assume that the spectrum of $x(t)$ can be written as $F(\omega)Y(\omega)$, then from (I-8),

$$F(s/c, \Delta_o) = \int_0^\infty Y^2(\omega'/c, \Delta_o)\, \bar{a}(s-\omega')\, d\omega' \Big/ Y^2(s/c, \Delta_o) \tag{I-9}$$

where everything on the right-hand side can be calculated from observations of $y(t)$ and $\hat{a}(\Delta)$. Then the spectrum of the unknown event at distance Δ_o is given by

$$X(\omega, \Delta_o) = F(\omega, \Delta_o) Y(\omega, \Delta_o).$$

Results for a particular form of $\hat{a}(\Delta)$

Suppose that

$$\hat{a}(\Delta) \approx G e^{-q\Delta}$$

where G and q are determined from a least-squares fit to the observations of $\hat{a}(\Delta)$. Then using this approximation in the left-hand side of (I-7), we get

$$G c^{-1} \int_0^\infty Y^2(\omega'/c, \Delta_0) \int_{\beta-i\infty}^{\beta+i\infty} e^{-(q+\omega')\Delta} e^{s\Delta} d\Delta \, d\omega'$$

$$= G c^{-1} \int_0^\infty Y^2(\omega'/c, \Delta_0) \, \delta(s-q-\omega') \, d\omega'$$

$$= G c^{-1} Y^2[(s-q)/c, \Delta_0]$$

Thus

$$X(\omega, \Delta_0) = GY^2[(\omega-q/c, \Delta_0]/Y(\omega, \Delta_0) \qquad (I-11)$$

Thus we can calculate the spectrum $X(\omega, \Delta_0)$, since we can evaluate the right-hand side of (I-11). As a check on the result (I-11), we see that if there is no change in $\hat{a}$ with distance (q=0), then $X(\omega, \Delta_0) = GY(\omega, \Delta_0) = \hat{a}(\Delta_0) Y(\omega, \Delta_0)$ implying that the spectra have the same shape - or equivalently, that their waveforms are identical. If there were no attenuation with distance (c= 0), then the method would fail, as can be seen by setting c = 0 in (I-6).

In practice, estimates of $g(\omega)$ would be obtained from the observed slope of $\log[Y(\omega, \Delta_0)/Y(\omega, \Delta)]$. Then the best linear approximation $(c\omega)$ to $g(\omega)$ could be determined. This would be

the preferable approach, since the total propagation losses comprising
both intrinsic absorption and scattering would be accounted for.

In summary, then, using equations (I-8) or (I-11) we have
a means of estimating the spectrum of the unknown event in terms
of the spectrum of y(t).

APPENDIX II

SURFACE WAVE SYNTHESIS

We have written a program which computes a synthetic surface wave seismogram from assumed group velocity and source radiation spectrum. The input parameters are:

T	Period in seconds.
C(T)	Phase velocity as a function of period.
A(T)	Source amplitude spectrum.
R	Epicentral distance.
T_1	Starting time $(R/U_{max}.)$.
DT	Time increment for synthesis output.
NP	Desired number of output points in synthetic seismogram.
DF	Frequency increment.

The synthesis is given by:

$$y(R,t) = 2\Delta\omega \sum_i \left[A(\omega_i) \cos \eta(\omega_i,t) \frac{\sin \beta(\omega_i,t)}{\beta(\omega_i,t)} \right. \qquad (\text{II-1})$$

$$\left. + \left(\frac{\partial A}{\partial \omega}\right)_{\omega_i} \frac{\Delta\omega \sin \eta(\omega_i,t)}{\beta(\omega_i,t)} \left(\cos \beta(\omega_i,t) - \frac{\sin \beta(\omega_i,t)}{\beta(\omega_i,t)} \right) \right]$$

where
$$\eta(\omega_i,t) = \omega_i \left[t - R/C(\omega_i) \right]$$
$$\beta(\omega_i,t) = \Delta\omega \left[t - R/U(\omega_i) \right]$$

$$U(\omega_i) = C(\omega_i)\left[1 - \frac{\omega_i}{C(\omega_i)}\left(\frac{dC(\omega)}{d\omega}\right)_{\omega_i}\right]^{-1} \quad \text{(group velocity)}$$

This is a generalization of the synthesis method devised by
Aki (Reference 2).

For a derivation of Equation (II-1), see Reference 3, pp. 139.
We convert input periods to frequency, and fit polymonials to the
input phase velocity and amplitude values, both to facilitate the
calculation of U(ω) and $\partial A/\partial \omega$, and to allow us to evaluate the
integrand in Equation (II-1) at equal increments of frequency.

DOCUMENT CONTROL DATA - R&D

(Security classification of title, body of abstract and indexing annotation must be entered when the overall report is classified)

1. ORIGINATING ACTIVITY (Corporate author)	2a. REPORT SECURITY CLASSIFICATION
TELEDYNE INDUSTRIES, INC.	Unclassified
EARTH SCIENCES DIVISION	2b. GROUP
ALEXANDRIA, VIRGINIA, 22314	--

3. REPORT TITLE

DETECTION OF SURFACE WAVES FROM SMALL EVENTS AT TELESEISMIC DISTANCES

4. DESCRIPTIVE NOTES (Type of report and inclusive dates)

Scientific Report

5. AUTHOR(S) (Last name, first name, initial)

Alexander, S. S.
Rabenstine, D. B.

6. REPORT DATE	7a. TOTAL NO. OF PAGES	7b. NO. OF REFS
1 March 1967	64	5

8a. CONTRACT OR GRANT NO.	9a. ORIGINATOR'S REPORT NUMBER(S)
AF 33(657)-15919	
b. PROJECT NO	
VELA T/6702	SDL Report No. 175
c.	9b. OTHER REPORT NO(S) (Any other numbers that may be assigned this report)
ARPA Order No. 624	
ARPA Program Code No. 5810	--

10. AVAILABILITY/LIMITATION NOTICES

This document is subject to special export controls and each transmittal to foreign governments or foreign national may be made only with prior approval of Chief, AFTAC.

11. SUPPLEMENTARY NOTES	12. SPONSORING MILITARY ACTIVITY
--	ADVANCED RESEARCH PROJECTS AGENCY
	NUCLEAR TEST DETECTION OFFICE
	WASHINGTON, D. C.

13. ABSTRACT

A matched filter approach for distinguishing weak teleseismic surface wave signals from background noise is presented. The method discriminates against events not located in a particular source region of interest and provides estimates of magnitude and radiation pattern, when a number of recording stations are available. Test cases and typical results for different source regions are discussed.

DD FORM 1 JAN 64 1473

14. KEY WORDS	LINK A		LINK B		LINK C	
	ROLE	WT	ROLE	WT	ROLE	WT
Matched Filter						
Surface Wave Analysis						
Source Mechanism						
Magnitude Estimates						

INSTRUCTIONS

1. ORIGINATING ACTIVITY: Enter the name and address of the contractor, subcontractor, grantee, Department of Defense activity or other organization (corporate author) issuing the report.

2a. REPORT SECURITY CLASSIFICATION: Enter the overall security classification of the report. Indicate whether "Restricted Data" is included. Marking is to be in accordance with appropriate security regulations.

2b. GROUP: Automatic downgrading is specified in DoD Directive 5200.10 and Armed Forces Industrial Manual. Enter the group number. Also, when applicable, show that optional markings have been used for Group 3 and Group 4 as authorized.

3. REPORT TITLE: Enter the complete report title in all capital letters. Titles in all cases should be unclassified. If a meaningful title cannot be selected without classification, show title classification in all capitals in parenthesis immediately following the title.

4. DESCRIPTIVE NOTES: If appropriate, enter the type of report, e.g., interim, progress, summary, annual, or final. Give the inclusive dates when a specific reporting period is covered.

5. AUTHOR(S): Enter the name(s) of author(s) as shown on or in the report. Enter last name, first name, middle initial. If military, show rank and branch of service. The name of the principal author is an absolute minimum requirement.

6. REPORT DATE: Enter the date of the report as day, month, year; or month, year. If more than one date appears on the report, use date of publication.

7a. TOTAL NUMBER OF PAGES: The total page count should follow normal pagination procedures, i.e., enter the number of pages containing information.

7b. NUMBER OF REFERENCES: Enter the total number of references cited in the report.

8a. CONTRACT OR GRANT NUMBER: If appropriate, enter the applicable number of the contract or grant under which the report was written.

8b, 8c, & 8d. PROJECT NUMBER: Enter the appropriate military department identification, such as project number, subproject number, system numbers, task number, etc.

9a. ORIGINATOR'S REPORT NUMBER(S): Enter the official report number by which the document will be identified and controlled by the originating activity. This number must be unique to this report.

9b. OTHER REPORT NUMBER(S): If the report has been assigned any other report numbers (either by the originator or by the sponsor), also enter this number(s).

10. AVAILABILITY/LIMITATION NOTICES: Enter any limitations on further dissemination of the report, other than those imposed by security classification, using standard statements such as:

(1) "Qualified requesters may obtain copies of this report from DDC."

(2) "Foreign announcement and dissemination of this report by DDC is not authorized."

(3) "U. S. Government agencies may obtain copies of this report directly from DDC. Other qualified DDC users shall request through

_____."

(4) "U. S. military agencies may obtain copies of this report directly from DDC. Other qualified users shall request through

_____."

(5) "All distribution of this report is controlled. Qualified DDC users shall request through

_____."

If the report has been furnished to the Office of Technical Services, Department of Commerce, for sale to the public, indicate this fact and enter the price, if known.

11. SUPPLEMENTARY NOTES: Use for additional explanatory notes.

12. SPONSORING MILITARY ACTIVITY: Enter the name of the departmental project office or laboratory sponsoring (paying for) the research and development. Include address.

13. ABSTRACT: Enter an abstract giving a brief and factual summary of the document indicative of the report, even though it may also appear elsewhere in the body of the technical report. If additional space is required, a continuation sheet shall be attached.

It is highly desirable that the abstract of classified reports be unclassified. Each paragraph of the abstract shall end with an indication of the military security classification of the information in the paragraph, represented as (TS), (S), (C), or (U).

There is no limitation on the length of the abstract. However, the suggested length is from 150 to 225 words.

14. KEY WORDS: Key words are technically meaningful terms or short phrases that characterize a report and may be used as index entries for cataloging the report. Key words must be selected so that no security classification is required. Identifiers, such as equipment model designation, trade name, military project code name, geographic location, may be used as key words but will be followed by an indication of technical context. The assignment of links, rules, and weights is optional.

GPO 886-551